ORGANIC PROCESS RESEARCH & DEVELOPMENT
OPR&D

pubs.acs.org/OPRD

Article

Optimized Synthesis of Indole Carboxylate Metallo-β-Lactamase Inhibitor EBL-3183

Andrei Baran,* Jevgenijs Kuzmins, Jevgenijs Kuznecovs, Alistair J. M. Farley, Tharindi Panduwawala, Anete Parkova, Pavel A. Donets, Jürgen Brem, Edgars Suna, Christopher J. Schofield,* and Kirill Shubin*

Cite This: *Org. Process Res. Dev.* 2023, 27, 692−706

Read Online

ACCESS | Metrics & More | Article Recommendations | Supporting Information

ABSTRACT: A new synthetic route for the preparation of the metallo-β-lactamase inhibitor pre-candidate EBL-3183 was developed and carried out on a kilogram scale. The described process starts from a commercially available indole-2-carboxylate and employs an Ellman auxiliary approach coupled with ruthenium-catalyzed stereoselective reduction for the introduction of chirality. The key spirocyclic cyclobutane motif was assembled utilizing an epoxide building block, which was conveniently obtained in diastereomerically pure form. The amount and quality of the prepared final target EBL-3183 were sufficient for the preclinical studies.

KEYWORDS: *metallo-β-lactamase inhibitor, indole carboxylates (InCs), epoxidation, Suzuki−Miyaura coupling, Ellman auxiliary, spiro cyclobutane, NDM-1, VIM-1*

INTRODUCTION

Antibacterial-resistant Gram-negative bacteria, including the "ESKAPE" pathogens, are major causes of healthcare-associated infections and death.[1] The most important drivers of resistance against carbapenems, often drugs of last choice for serious Gram-negative infections, involve production of carbapenemases, including metallo-β-lactamases (MBLs).[2] In contrast to the serine β-lactamases, few MBL inhibitors with real potential for clinical development have been reported and even fewer with the breadth of potency against the three major classes of MBLs, namely, NDM, IMP, and VIM variants, that is likely required for widespread clinical use.[3] Recently, we reported on a novel indole carboxylate (InC) scaffold useful for broad-spectrum MBL inhibition.[4] The best-performing compound **1** (Figure 1) displayed excellent *in vitro* and *in vivo* activity but was nonoptimal in safety studies prompting us to investigate analogues (data on the activities will be published elsewhere). A close *N*-analogue of InC **1**, i.e., InC **2**,[5] showed similarly good potentiation of carbapenems compared to **1**, though manifested improved *in vivo* properties. Consequently, InC **2** has progressed to preclinical studies.

To that end, we required a reliable scale-up procedure capable of supplying sufficient quantities of **2**. The medicinal chemistry route developed for the synthesis of **2** (Scheme 1) starts from ethyl 7-bromoindol-2-carboxylate **3** and progresses via modifications at C7 to the key chiral building block **9**.[5] Condensation of **9** with the epoxide *trans*-**16** introduces the spiro-fused cyclobutane-oxazolidinone motif and subsequent Suzuki−Miyaura coupling installs the C3 substituent. While the linear sequence from **3** to **2** appeared to be scalable, preparation of the cyclobutane building block *trans*-**16** employed preparative chiral HPLC separation of the corresponding epimeric mixture **16** and posed the linchpin problem to solve. An additional consideration was that the scale-up route to **2** preferably should support the ongoing medicinal chemistry program. In particular, different C3-substituted structures were required to obtain analogues of **2** for screening as backup compounds. Since the C3 group is introduced at the late stage in the medicinal chemistry route, via intermediate **11**, we decided to adopt the developed scheme as a blueprint for scale-up studies.

RESULTS AND DISCUSSION

Synthesis of the Chiral Building Block 9. As anticipated, the initial two steps of the route to 7-acetyl-3-bromo InC **5** from ethyl 7-bromoindol-2-carboxylate **3** could be smoothly transferred to the requisite scale with minor adjustments (Scheme 2). Thus, Heck reaction of **3** with *n*-butyl vinyl ether delivered an intermediate enol ether, which was hydrolyzed *in situ* to give acetyl derivative **4**. The original conditions were reproduced on a 1 kg scale; polishing filtration through a silica plug afforded sufficiently purified InC **4** in 89% yield. Subsequent bromination with NBS in MeCN followed by an optimized workup procedure provided **5** in 94% yield. Direct precipitation of **5** from the reaction mixture by 5% aq. $Na_2S_2O_3$ was simpler than the previously employed extractive procedure[4,5] and improved the product purity.

A significant bottleneck for implementation of the medicinal chemistry route on a larger scale was identified during the exploratory reduction of (*R*)-**7** with L-selectride. In addition to

Received: January 2, 2023
Published: March 30, 2023

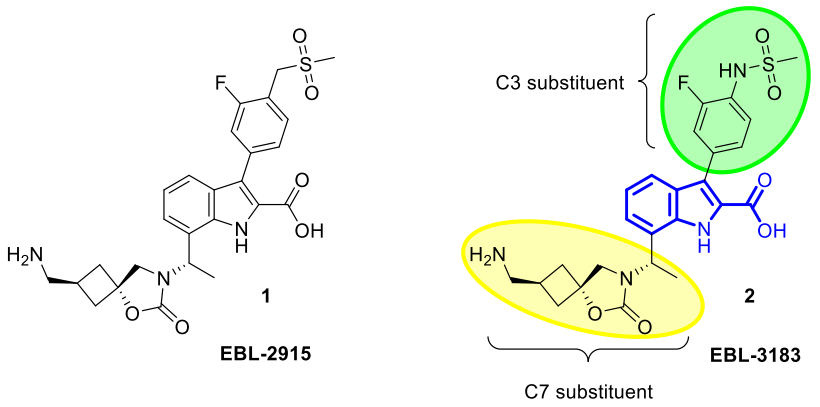

Figure 1. Structure of indole carboxylate metallo-β-lactamase inhibitors InC **1** (EBL-2915) and InC **2** (EBL-3183).

Scheme 1. Medicinal Chemistry Route to InC 2 (EBL-3183)[5]

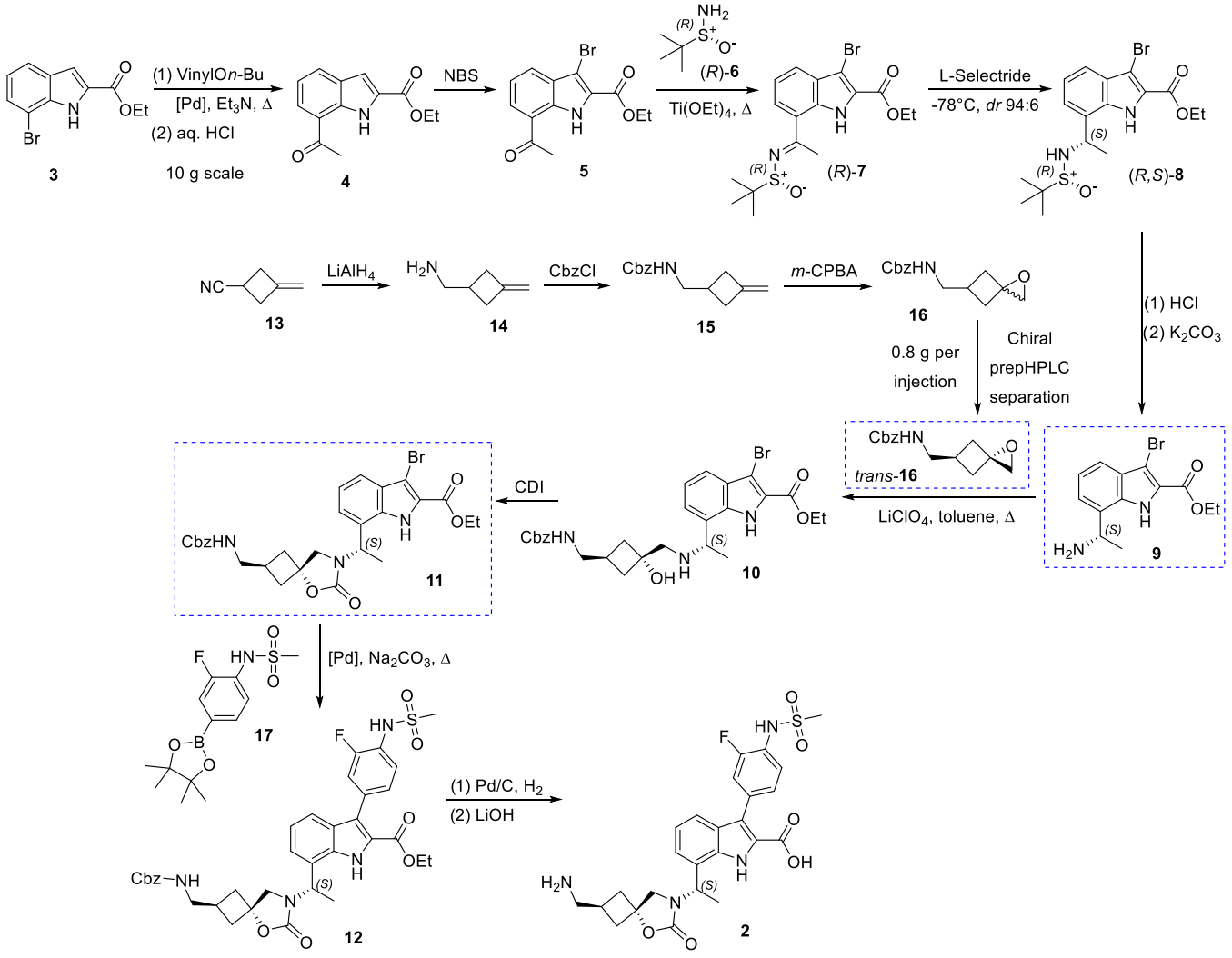

cryogenic conditions, this step required oxidative cleavage of liberated *sec*-Bu_3B. Although the reaction temperature could be increased to −50 °C from the originally used −78 °C with only marginal deterioration of dr (93:7 vs 94:6), the unwanted diastereomer still had to be separated chromatographically due to the low crystallinity of the (*R*,*S*)-**8** product (Scheme 3).

We searched for alternative more selective reductants and catalytic conditions, which would obviate the need for cryogenic temperature and an oxidative workup. Reduction by silanes[6] in the presence of Zn-salts and Ru-catalyzed transfer hydrogenation[7] were briefly tested as appropriate variants and both promisingly demonstrated capacity to deliver a dr ≥99:1. The selectivity of these methods is opposite to that of L-selectride and the corresponding diastereomer (*R*,*R*)-**8** is highly crystalline, which conveniently expanded the purification options. Therefore, the sulfinyl imine (*S*)-**7** was selected as

https://doi.org/10.1021/acs.oprd.3c00002
Org. Process Res. Dev. 2023, 27, 692−706

Scheme 2. Synthesis of the Bromide 5[a]

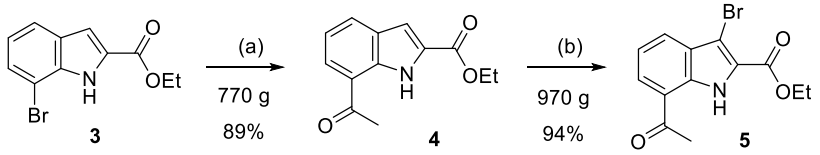

[a]Reagents and conditions (a), (1) vinylO*n*-Bu, $Pd(OAc)_2$ (3 mol %), dppp (6 mol %), Et_3N, EtOH, reflux, 20 h, and (2) 4 M aq. HCl, THF/DCM, 23 °C, 1 h; (b) NBS, MeCN, from 0 to 23 °C, 2 h.

Scheme 3. Preliminary Stereoselective Reduction of the Sulfinyl Imine (*R*)-7[a]

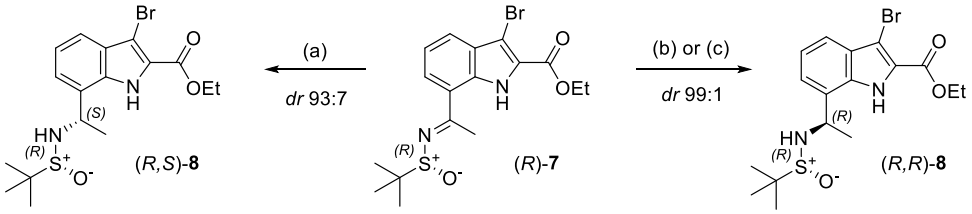

[a]Reagents and conditions (a) L-selectride, THF, −50 °C, 3 h; (b) $(EtO)_3SiH$ (10 equiv), $ZnBr_2$ (3 equiv), THF, 23 °C, 12 h, conversion 35%, dr 99:1; (c) $[RuCl_2(p\text{-cymene})]_2$ (2.5 mol %), 2-amino-2-methyl-1-propanol (5.0 mol %), *t*-BuOK (12.5 mol %) *i*-PrOH, reflux, 1 h, conversion 100%, dr >99:1.

Scheme 4. $Ti(OEt)_4$-Promoted Synthesis of the Sulfinyl Imine (*S*)-7[a]

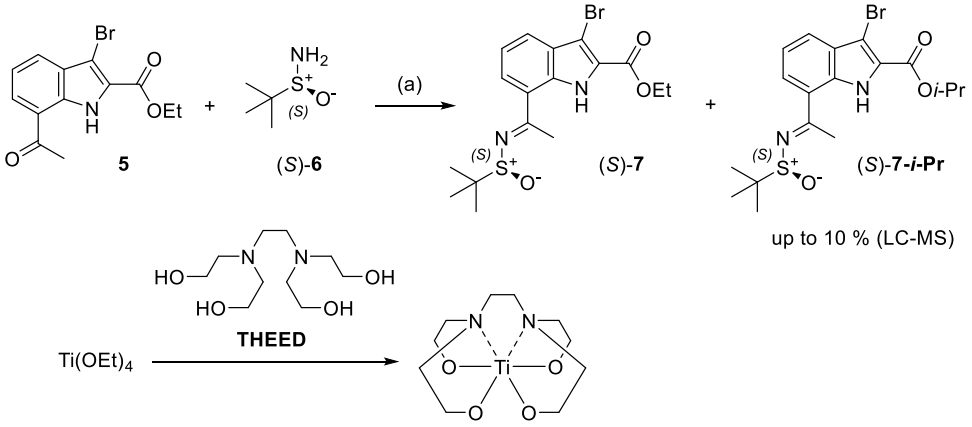

[a]Reagents and conditions (a): $Ti(OEt)_4$ + $Ti(O\text{i-Pr})_4$ (10−15 wt %), THF, reflux, 10 h.

Scheme 5. Synthesis of the Chiral Building Block 9[a]

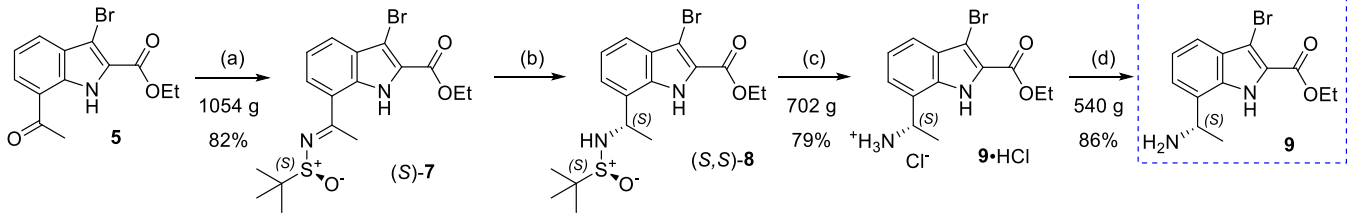

[a]Reagents and conditions: (a), (1) (*S*)-(−)-2-methyl-2-propanesulfinamide (*S*)-**6**, $Ti(OEt)_4$, Dean−Stark apparatus, THF, reflux, 26 h, and (2) THEED, 50 °C, 45 min; (b) $[RuCl_2(p\text{-cymene})]_2$ (2 mol %), 2-amino-2-methyl-1-propanol (4 mol %), *t*-BuOK (10 mol %), *i*-PrOH, reflux, 1 h; (c) 4 M HCl/dioxane, EtOH/THF, from 0 to 23 °C, 1 h; (d) Na_2CO_3, DCM/H_2O, 23 °C, 20 h.

a suitable substrate for the large-scale installation of the requisite (*S*)-stereocentre.

Synthesis of (*S*)-**7** was carried out using a standard approach, wherein the reaction is promoted by $Ti(OEt)_4$, which acts both as a Lewis acid activator and a dehydrating agent (Scheme 4).[8] However, most of the commercially available $Ti(OEt)_4$ contains a significant amount of $Ti(O\text{i-Pr})_4$ (up to 10−15 wt %), which was found to effect formation of an impurity (*S*)-**7-*i*-Pr** by transesterification of InC (*S*)-**7**. Hence, the quality of the titanium reagent had to be strictly controlled.

Slow condensations of Ellman's sulfinamide **6** with ketones are accelerated by the removal of the liberated alcohol allowing for higher conversion and yield.[8b] Therefore, EtOH was continuously expelled by distillation as a THF azeotrope[9] (bp 66 °C with 6 wt % of EtOH). During the entire reaction time,

https://doi.org/10.1021/acs.oprd.3c00002
Org. Process Res. Dev. 2023, 27, 692−706

Scheme 6. Alternative Methods for the Preparation of Epoxide 16 and Surrogates 16a−c[a]

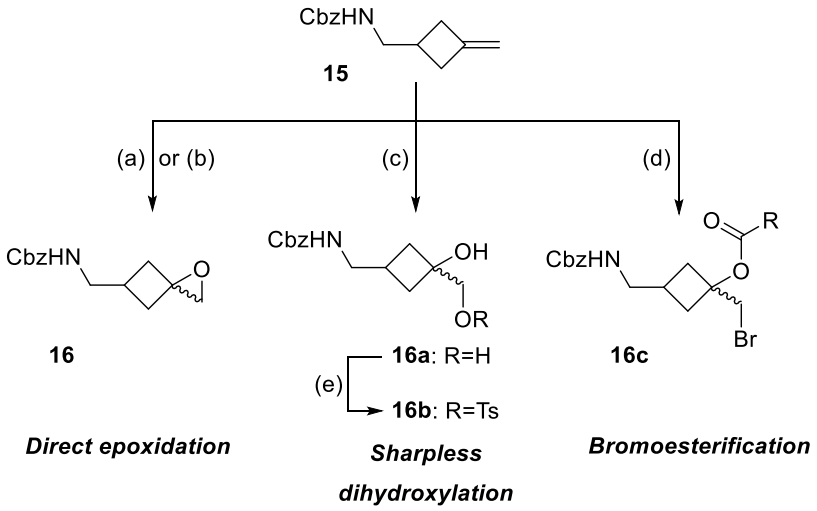

[a]Reagents and conditions: (a) ketone, Oxone, $NaHCO_3$, solvent/H_2O; (b) *metal* **cat-1-5**, oxidant, solvent; (c) AD-mix-α or β, *t*-BuOH/H_2O; (d) R−CO_2H, NBS, 2,6-lutidine, DCM; (e) TsCl, pyridine.

Table 1. Direct Epoxidation of Alkene 15

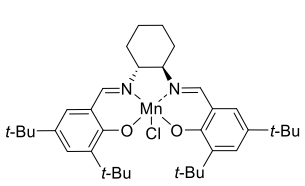

cat-1
(R,R)-Jacobsen catalyst

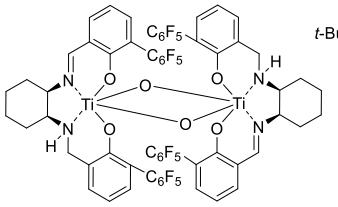

cat-2
Berkessel-Katsuki catalyst

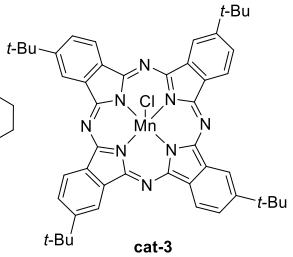

cat-3
White-Paradine catalyst

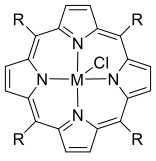

cat-4 (M = Fe, R = Ph)
cat-5 (M = Mn, R = Mes)

entry	conditions	yield of **16**	*trans*/*cis* (^{1}H NMR)
1	acetone, $NaHCO_3$, EtOAc, H_2O, rt, 1 h[a]	76%	50:50
2	trifluoroacetone, $NaHCO_3$, EtOAc, H_2O, rt, 24 h[a]	no reaction	
3	trifluoroacetophenone, $NaHCO_3$, EtOAc, H_2O, rt, 24 h[a]	no reaction	
4	D-epoxone, $NaHCO_3$, EtOAc, H_2O, rt, 24 h[a]	no reaction	
5	D-epoxone, $NaHCO_3$, MeCN, H_2O, rt, 1 h[a]	62%	50:50
6	trifluoroacetone, $NaHCO_3$, MeCN, H_2O, rt, 1 h[a]	74%	50:50
7	trifluoroacetophenone, $NaHCO_3$, MeCN, H_2O, rt, 1 h[a]	81%	50:50
8	**cat-1**, NaOCl, aq. Na_2HPO_4 (pH 11), DCM, 4 °C, 6 h	33%	37:63
9	***ent*-cat-1**, NaOCl, aq. Na_2HPO_4 (pH 11), DCM, 4 °C, 6 h	36%	40:60
10	**cat-2**, NBu_4HSO_4, H_2O_2, DCE, rt, 16 h	67%	15:85
11	**cat-3**, PhIO, DCM, rt, 16 h	66%	33:67
12	**cat-4**, PhIO, DCM, rt, 16 h	50%	43:57
13	**cat-5**, PhIO, DCM, rt, 16 h	28%	67:33

[a]In the presence of Oxone.

an inert atmosphere was maintained and 1 L of distillate was collected on a 1 kg scale.

A common complication in titanium-promoted reactions stems from the formation of titanium hydroxide gel during aqueous workup. Usually, this is converted to a filterable solid upon quenching with 24 wt % aq. NaCl, but the procedure is not always efficient.[8] The addition of Celite can help to decrease time of filtration,[8b,c] though an improved approach involves conversion of titanium alkoxides to a water-soluble ligand-bound form.[10] Thus, addition of *N,N,N′,N′*-tetrakis(2-hydroxyethyl)ethylenediamine (**THEED**) prior to reaction quenching greatly simplified extraction using the EtOAc/water system and enhanced separation of the phases. Final purification of the imine (*S*)-**7** was accomplished by filtration through a silica plug resulting in an overall 82% yield.

With sufficient (*S*)-**7** at our disposal, we then focused on the elaboration of the previously tested provisional reduction conditions (Scheme 3b,c) to complete the synthesis of the key intermediate **9** (Scheme 5). Extensive screening[11] of silane/Zn-salt combinations identified the $(EtO)_3SiH/ZnI_2$ couple as the most efficient silane-based system. While these conditions afforded high stereoselectivity (dr 96:4 to 99:1), the required large excess of the silane rendered the method unusable for scale-up.

On the other hand, Ru-catalyzed transfer hydrogenation proved to be the method of choice. Indeed, reduction of (*S*)-**7**

https://doi.org/10.1021/acs.oprd.3c00002
Org. Process Res. Dev. 2023, 27, 692−706

can be carried out at a moderately elevated temperature, does not require a high catalyst loading, and is readily scalable; indeed, 1 kg scale reduction of (*S*)-**7** was accomplished with de >99%. The reaction workup is straightforward: after concentration of the reaction mixture to half the original volume, the residue was dissolved in EtOAc, filtered through silica, and then concentrated. Some dark-colored unidentified impurities present in the product had no apparent influence on the following steps and the obtained crude material was used without additional purification.

Sulfinamide (*S*,*S*)-**8** was hydrolyzed using HCl in dioxane and THF/EtOH (2:1 v/v) as the solvent. The crude product was slurried in MTBE to provide the hydrochloride **9**·HCl, in 79% yield; the corresponding free base **9** was obtained after extraction between sat. aq. Na_2CO_3 and DCM. The crystalline amine **9** is a convenient staging point, where thorough removal of impurities is possible. Thus, recrystallization from heptane/EtOAc mixture provided **9** of ≥99% purity on a 0.5 kg scale. The exact configuration of the obtained derivative was confirmed by comparing the optical rotation value of the hydrochloride **9**·HCl with the corresponding data given in the literature,[5] showing full correspondence.

Synthesis and Incorporation of the Cyclobutane Building Block. A key element of a practical large-scale synthesis of the target InC **2** according to the medicinal chemistry route (Scheme 1) is the scalable stereoselective preparation of the key spirocyclic cyclobutane-epoxide *trans*-**16**. The latter ultimately originates from commercially available 3-methylidene-cyclobutane-1-carbonitrile **13**, which is transformed into the epoxidation precursor **15** via a two-step reduction−protection sequence. Since the reported[4] epoxidation of **15** with *m*-CPBA in DCM affords an ∼1:1 ratio of *trans*/*cis* mixture of epoxide **16**, we undertook a survey of alternative oxidation conditions in a search for stereoselectivity (Scheme 6).

Initially, epoxidation of alkene **15** was attempted with *in situ* generated dioxirane using Oxone as the terminal oxidant and catalytic acetone. Gratifyingly, good reactivity was observed and **16** was isolated in 76% yield (Table 1, entry 1), albeit without diastereocontrol. A limited investigation of alternative ketones, including enantiopure D-epoxone, did not improve the diastereoselectivity of the reaction (Table 1, entries 2−7).

Metal-catalyzed epoxidation methods were examined next. Thus, reaction with (*R*,*R*)-Jacobsen's catalyst **cat-1** using NaOCl as the oxidant delivered the epoxide **16** in 33% yield and 37:63 dr in favor of the *cis*-**16** (Table 1, entry 8). The corresponding (*S*,*S*)-catalyst ***ent*-cat-1** afforded the same major diastereomer, as anticipated (Table 1, entry 9). Interestingly, the *cis*-cyclohexylamine-derived dimeric titanium complex **cat-2** displayed an even higher preference for the formation of the undesired *cis*-**16** (Table 1, entry 10). Subsequently, Mn- and Fe-based phthalocyanine and porphyrin catalysts **cat-3** to **cat-5** were trialed using iodosylbenzene as the oxidant; while **cat-5** showed modest levels of stereoselectivity for *trans*-**16**, the yield was poor (Table 1, entries 11−13). At this stage, we decided to explore alternative methods of preparing *trans*-**16**, because the tested direct epoxidation reactions had failed to deliver the requisite selectivity, would likely not be amenable to ready scale up, and required preparative HPLC purification using a chiral column, which has been previously identified[5] as the sole adequate separation technique.

To investigate options for the separation of the isomers by less expensive silica gel flash chromatography, cyclobutanes **16b** and **16c** were prepared. Dihydroxylation of **15** with AD-mix-α and β provided diols **16a** as an inseparable 60:40 mixture (Table 2). Tosylation of the latter afforded alcohols **16b** with the same dr and failed to resolve the separation issue.

Table 2. Dihydroxylation of Alkene 15

entry	conditions	yield of **16a** (%)	dr (^{1}H NMR)[a]
1	AD-mix-α, *t*-BuOH/H_2O (1:1), rt, 20 h	96	60:40
2	AD-mix-β, *t*-BuOH/H_2O (1:1), rt, 20 h	82	60:40

[a]The configuration of major/minor diastereomers was not determined.

Next, several bromo esters **16c** were prepared and tested in separation (Table 3). Unfortunately, bromoesterification of **15** was also found to be largely unselective and the resulting diastereomers were inseparable. A consistent absence of substantial substrate control (dr 50:50 to 60:40) was observed in all the tested oxidations of **15** and it was concluded that the desired selectivity could not be obtained by the employed reagents. These unpromising results prompted us to look for an alternative building block that could be integrated into the synthetic route without major modification.

Table 3. Bromoesterification of Alkene 15[a]

Entry	R	Yield of **16c**	*dr* (^{1}H NMR)[b]
1	Me-	25%	60:40
2	$HOCH_2$-	36%	50:50
3	Ph_2CH-	27%	50:50
4		31%	57:43

[a]NBS, 2,6-lutidine, DCM, 20 h, rt. [b]The configurations of the major/minor diastereomers were not determined.

It was proposed that the nitrile of **13** may act as a suitable masking group for the aminomethyl moiety residing in the final InC **2** (Scheme 7)[12] and that unmasking reduction could be carried out at the same stage as the Cbz-deprotection. Hence, there is formal equivalence between the nitrile **11′** and the originally planned Cbz-protected intermediate **11**. Use of the new cyclobutane building block *trans*-**16′** would also shorten the entire synthetic scheme by two Cbz-protection/deprotection steps. Small-scale (<1 g) preparation of the requisite epoxide *trans*-**16′** via direct oxidation of **13** has been described,[13] and it was envisaged that this could be used as a starting point for our scale-up efforts.

We therefore attempted to reproduce the synthesis of *trans*-**16′** using the reported[13] epoxidation procedures: with peroxyimidic acid **18** generated *in situ* from trichloroacetonitrile/H_2O_2, and with *m*-CPBA (Table 4). Contrary to the described outcome, the experiment with **18** led to poor diastereoselectivity (*trans*/*cis*-**16′** 65:35 vs published[13] 95:5), while the conversion reached only 76% after 8 h with 2.0 equiv of H_2O_2. Moreover, multiple byproducts were detected in the reaction mixture (Table 4, entry 1).

https://doi.org/10.1021/acs.oprd.3c00002
Org. Process Res. Dev. 2023, 27, 692−706

Scheme 7. Alternative Cyclobutane Building Block—Cyano Epoxide *trans*-16′[a]

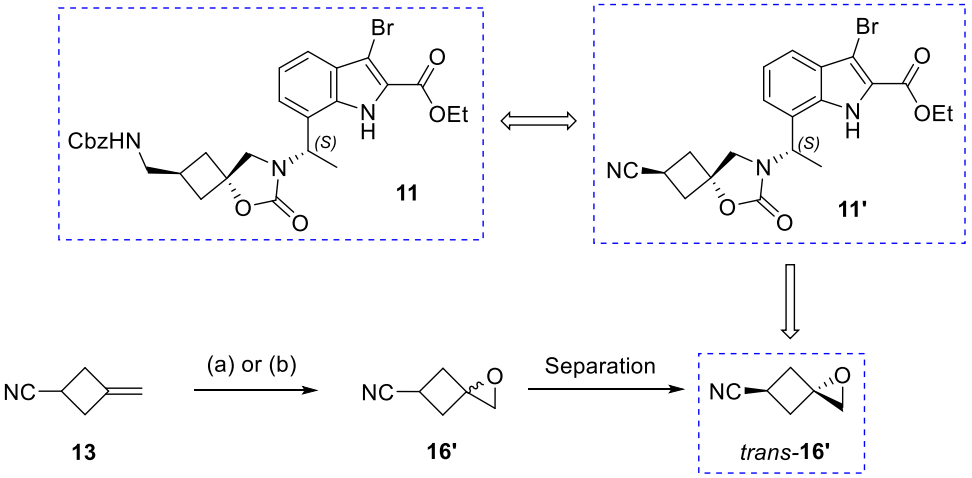

[a]Reagents and conditions: (a) $Cl_3CC(NH)OOH$ **18** (2 equiv), DCM, 20 °C, 2 h; (b): *m*-CPBA (1.2 equiv), DCM, from 0 to 20 °C, 1 h.

Table 4. Epoxidation of Alkene 13[a]

entry	oxidant	solvent	addition	time (h)	temp. (°C)	conv. (%)	*trans*/*cis*
1	$Cl_3CCN + H_2O_2$[b]	DCM	direct	8	23	76	65:35
2	*m*-CPBA[b]	DCM	direct	16	0−23	91	70:30
3	*m*-CPBA[c]	DCM	direct	16	0−23	100	72:28
4	*m*-CPBA[c]	DCM	inverse	16	0−23	100	79:21
5	*m*-CPBA[c]	THF	inverse	16	0−23	70	77:23
6	*m*-CPBA[c]	toluene	inverse	16	0−23	100	81:19

[a]All reactions were carried out on ∼1 g scale; conversion determined by GC−MS assay; dr by GC−MS and $^{13}C\{^1H\}$ NMR. [b]Pre-conditioned[13] *m*-CPBA (1.2 equiv) was used, dilution 85 mL per 1 g of **13**. [c]Commercial 70−75% *m*-CPBA (1.2 equiv) was used, dilution 30 mL per 1 g of **13**.

Oxidation with *m*-CPBA (1.2 equiv) afforded slightly better results with clean 91% conversion to **16′** with an approximate *trans*/*cis* 70:30 ratio (Table 4, entry 2). The major isomer of **16′** was assigned the requisite *trans* configuration based on the reported NMR data.

The original method[13] recommends complicated conditioning of commercial 70−75% grade *m*-CPBA with the purpose of purging the *m*-chlorobenzoic acid impurity. On the other hand, a near-identical result to that reported (*trans*/*cis* 74:26) was obtained with untreated *m*-CPBA at a higher concentration (Table 4, entry 3). Unexpectedly, measurable enhancement of selectivity was achieved when the order of reagent addition was inversed: dropwise addition of **13** to a solution of *m*-CPBA in DCM resulted in dr 79:21 (Table 4, entry 4).

The effect of the solvent (DCM, THF, or toluene) on the oxidation performance was next studied. The most nonpolar and industrially acceptable toluene led to slightly better results in terms of conversion and diastereoselectivity (Table 4, entry 6), therefore, was chosen for further elaboration. Under these conditions, an acceptable *trans*/*cis*-**16′** ratio of 81:19 was typically achieved.

An important aspect of the described procedures comprised the correct interpretation of analytical data for the assessment of diastereoselectivity of **16′**. GC−MS analysis of the reaction mixtures displayed wide variation in the apparent isomeric ratios depending on the sample concentration.[14] Therefore, an alternative independent control method was required. While ^1H NMR (400 MHz) spectra of the reaction mixture lacked the requisite resolution, the corresponding $^{13}C\{^1H\}$ NMR (101 MHz) spectra manifested two distinct sets of signals. Assuming the same spin relaxation pattern for both diastereomers, the selectivity was calculated as a ratio of the summed integration for ^{13}C peaks of the major component to the summed integration of the minor one. This approach conveniently allowed us to avoid lengthy quantitative inverse-gated $^{13}C\{^1H\}$ NMR measurements.[15] The obtained results are comparable with those obtained by GC−MS at the highest sample concentration. Therefore, we recommend using both $^{13}C\{^1H\}$ NMR and GC−MS to assess the diastereoselectivity of the epoxidation reaction giving **16′**.

The mixture of isomers **16′** obtained in the reaction of **13** with *m*-CPBA was subjected to vacuum distillation through a vacuum-jacketed Vigreux column (45 cm) with a boiling point range of 62−65 °C at 3 mbar. Gratifyingly, the desired *trans*-**16′** was distilled first and was collected in the main fraction. After the excess of *trans*-**16′** had been collected, an equimolar *trans*/*cis* mixture was obtained. Despite being described as a liquid,[13] freshly distilled *trans*-**16′** crystallized upon storage at +5 °C. Measurements with a controlled cooling manifested a melting point in the 29.5−32.5 °C range. It was also found that *trans*-**16′** readily crystallizes from a concentrated EtOAc solution upon cooling, which led to a major advancement in the separation of the target compound from the unwanted *cis* isomer. Indeed, if the crude product after epoxidation was extracted with EtOAc and concentrated to the final EtOAc/epoxide ratio 3:1 (v/v), crystallization of *trans*-**16′** isomer took place at −20 °C with 40% yield. Material prepared this way was free from *cis*-**16′** but contained residual solvents and minor impurities. The latter were removed by subsequent short path vacuum distillation affording the target epoxide *trans*-**16′** with 98−100% purity.

https://doi.org/10.1021/acs.oprd.3c00002
Org. Process Res. Dev. 2023, 27, 692−706

Scheme 8. Opening of the Epoxide *trans*-16′ with the Chiral Amine 9[a]

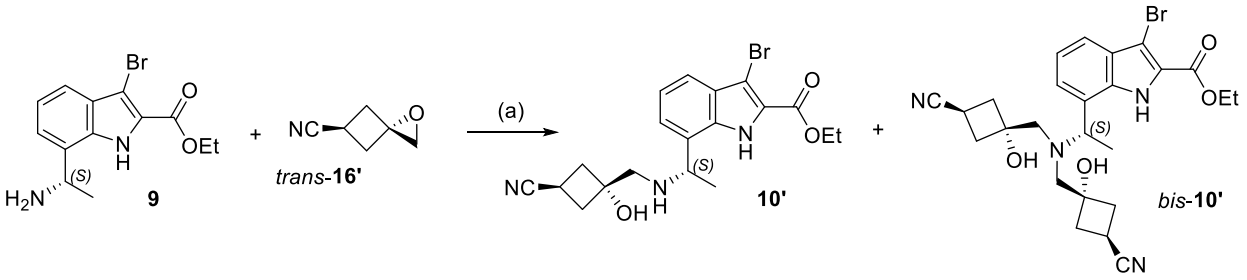

[a]Reagents and conditions: (a) solvent, temperature, open/sealed reaction vessel.

Table 5. Optimization of the Epoxide *trans*-16′ Opening with the Amine 9[a]

						LC-MS assay (%)		
entry	solvent	temp.	setup	time (h)	*trans*-16′ (equiv)	conv.	10′	*bis*-10′
1	EtOH	85 °C	A	24	1.4	100%	92	3
2	EtOH	reflux	B	48	1.4	0%		
3	toluene	reflux	B	48	1.4	<10%	1	10
4	toluene/*t*-AmOH (3:1 v/v)	reflux (102 °C)	B	6	1.4	100%	89	5
5	toluene/*t*-AmOH (3:1 v/v)	reflux (102 °C)	B	72	1.0[b]	0%		

[a]Reactions were carried out with 0.5 g of **9** at 10:1 v/wt dilution: A—in a pressure tube, B—in a flask with a reflux condenser. [b]Reaction with the Cbz-protected analogue *trans*-**16**.

Scheme 9. Synthesis of Building Block *trans*-16′ and Intermediate 11′[a]

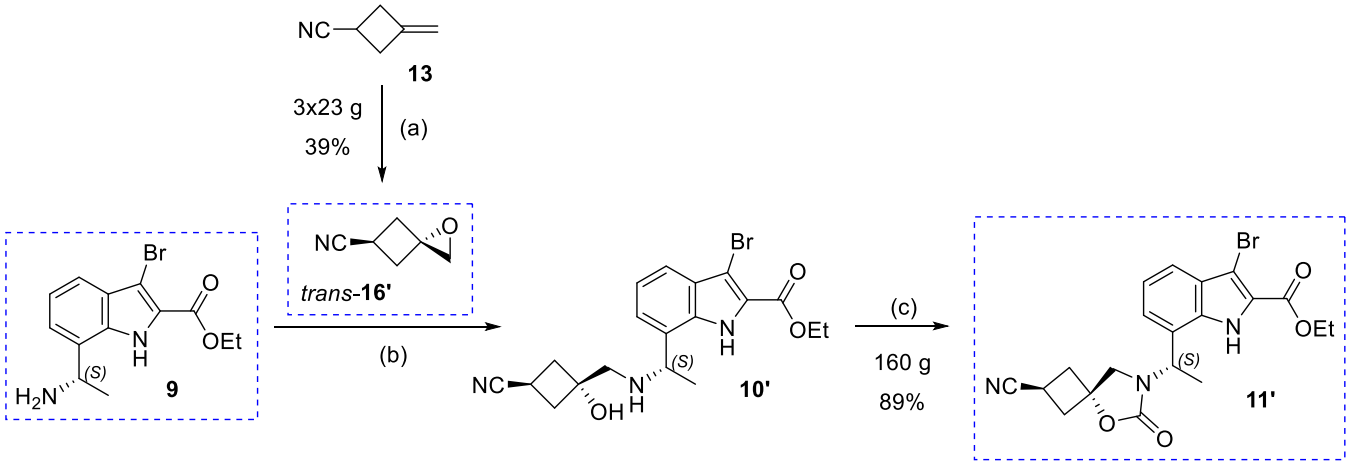

[a]Reagents and conditions: (a) *m*-CPBA, toluene, from 0 to 23 °C, 16 h; crystallization; distillation; (b) toluene/*t*-AmOH, reflux, 18 h; (c) CDI, MeCN, 23 °C, 18 h.

The described oxidation-crystallization sequence was carried out in three 50 g batches of **13**, with each batch providing 30–34 g of *trans*-**16′** with dr ≥98:2. Concluding short path distillation resulted in 22–23 g (38–40%) yields of pure *trans*-**16′**. All three batches were pooled to provide total 67.8 g (39%) of the building block *trans*-**16′** with a final dr of 99:1. The stereochemistry of the obtained product was additionally confirmed by transformation to the Cbz-protected aminomethyl epoxide *trans*-**16**.[16]

With the two key building blocks **9** and *trans*-**16′** in hand, we addressed the next step of epoxide opening (Scheme 8). The conditions from the medicinal chemistry route (heating in toluene with $LiClO_4$ in a sealed reaction vessel)[4,5] were used as a starting point. However, formation of a significant amount of *bis*-**10′** and lack of reproducibility due to hygroscopicity of $LiClO_4$ forced us to look for a better alternative.

Thus, it was discovered that reaction of *trans*-**16′** in protic solvents (EtOH or *i*-PrOH) proceeded with an equally high conversion without the need for a Lewis acidic promoter.[17] In this case, the ratio of target ethanolamine **10′** and side-product *bis*-**10′** could be adjusted by the excess of the epoxide *trans*-**16′** added.

Another deficiency of the original method[4,5] surfaced with switching of the reaction setup from a sealed vessel to atmospheric pressure conditions (Table 5). Heating of **9** and *trans*-**16′** in EtOH at 85 °C in a closed system resulted in complete conversion after 24 h in the presence of 1.4 equiv of epoxide (Table 5, entry 1). However, the same reaction at reflux in an open system did not produce any conversion after 48 h (Table 5, entry 2). Lack of reactivity was also observed in refluxing toluene, where the bis-adduct *bis*-**10′** was formed predominantly (Table 5, entry 3). However, the introduction of a protic high-boiling *tert*-amyl alcohol (*t*-AmOH) as a co-

https://doi.org/10.1021/acs.oprd.3c00002
Org. Process Res. Dev. 2023, 27, 692–706

Scheme 10. Synthesis of the Target InC 2 from the Intermediate 11′[a]

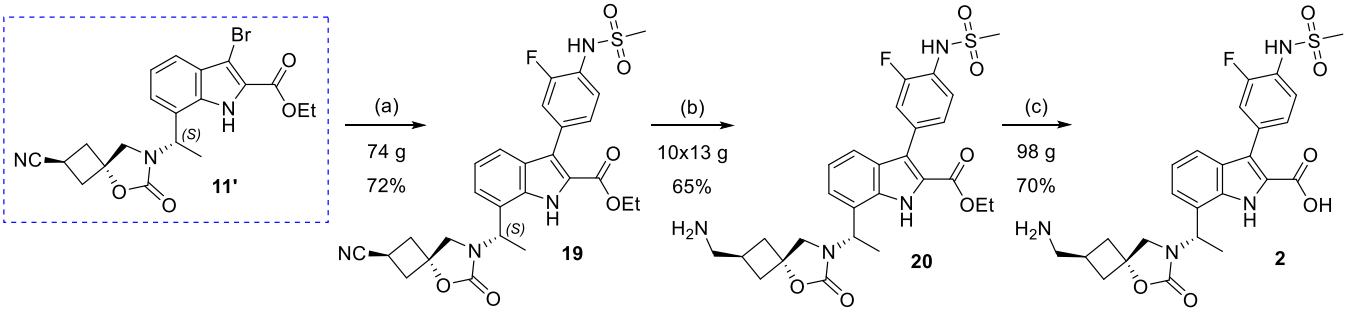

[a]Reagents and conditions: (a): boronate **17**, $Pd(dppf)Cl_2 \cdot CH_2Cl_2$ (5 mol %), Na_2CO_3, 1,4-dioxane/H_2O, 80 °C, 3.5 h; (b) H_2 (50 bar), Raney-Ni (50 wt %), 25% aq. NH_4OH, THF, 50 °C, 16 h; (c) LiOH, THF/H_2O, from 0 to 23 °C, 40 h.

Scheme 11. Reduction of the Nitrile 19[a]

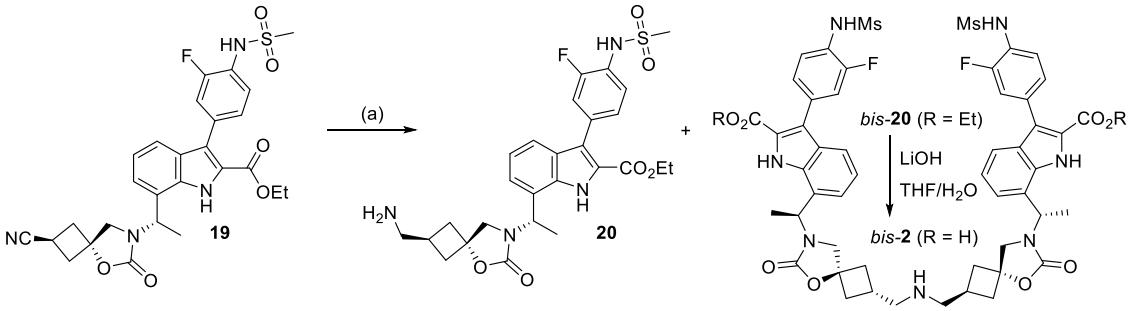

[a]Reagents and conditions: (a) H_2 (50 bar), Raney-Ni, THF/25−28% NH_4OH, 50 °C, 16 h.

solvent led to complete consumption of **9** in 6 h at reflux with an acceptable **10′**/*bis*-**10′** ratio (Table 5, entry 4). Interestingly, the nitrile group of *trans*-**16′** appears to enhance the electrophilicity of the spiro cyclobutane-epoxide scaffold, since the aminomethyl analogue *trans*-**16** did not react under the optimal conditions (Table 5, entry 5).

On the final 125 g scale, complete conversion of **9** was reached with only 1.1 equiv of the epoxide *trans*-**16′** and the ratio of **10′**/*bis*-**10′** was improved to 97:3 (Scheme 9).

The crude oily ethanolamine **10′** is difficult to purify by extraction or crystallization. Therefore, the oil was used directly in the following cyclization stage, whereupon crystalline oxazolidinone **11′** is formed. According to the original method, the cyclization was effected by CDI in MeCN with 89% yield over two stages.

Installation of the C3 Substituent and the Endgame. Following the development of a reliable technology for the preparation of intermediate **11′** (Scheme 9), installation of the C3 substituent to give the target InC **2** was carried out analogously to the medicinal chemistry route (Scheme 10). The original conditions for the Suzuki−Miyaura cross-coupling were readily scaled up without major modifications to 84 g of the bromide **11′**. Upon reaction with the boronate **17**,[18] the corresponding product **19** was simply precipitated from the concentrated extraction solution.

Reduction of the nitrile **19**, on the other hand, turned out to be more demanding than expected (Scheme 11). Although the $NaBH_4/NiCl_2$ system afforded the amine **20**, upscaling of this reaction was problematic.[19] Hydrogenation of **19** over Raney-Ni was identified as a more promising method for this transformation.

A typical side-reaction,[20] wherein a partially reduced nitrile reacts with the product to form a dimer, i.e., *bis*-**20**, was the main obstacle in the preparation of pure **20**. Saturation of the reaction medium with ammonia substantially suppressed this process and provided selectivity sufficient for practical large-scale use. The highest yield of 65% was obtained under 50 bar pressure at 50 °C, over 16 h with 5−7% content of the dimer *bis*-**20** (by peak area HPLC-UV analysis). Due to instrumental limitations, the hydrogenation of **19** was carried out in ten 20 g batches. Upon purging of ammonia from the crude product mixture, the amine **20** readily crystallized from alcoholic media. Unfortunately, the low solubility of the formed crystalline phase impeded complete removal of the dimer *bis*-**20** by an additional crystallization.

Therefore, crude **20** was used in the final hydrolysis step. While LiOH in aqueous THF smoothly effected the requisite saponification, the subsequent purification was subjected to optimization. Apparently, target InC **2** exists predominantly in a crystalline betaine form, which is insoluble in common organic solvents. On the other hand, InC **2** could be dissolved in aq. AcOH or aq. ammonia. Consequently, two principal purification methods were developed: precipitation using an antisolvent for acidic solutions or precipitation under pH-controlled conditions for basic solutions.

Various antisolvents were tested, e.g., EtOH, *i*-PrOH, and acetone; all were equally effective with regard to the obtained yield. The use of alcohols, however, resulted in the formation of a precipitate with better filterability. This method was found to be effective for the removal of all impurities, except for the dimer *bis*-**2** corresponding to the hydrolysis of *bis*-**20** impurity (Scheme 11). Accordingly, **2** could be obtained with only ~90% (HPLC-UV) purity as a stable solvate containing 0.75 equiv of EtOH.

Alternatively, pH-controlled precipitation was performed starting from an ammonium salt. Thus, crude **2** was dissolved

https://doi.org/10.1021/acs.oprd.3c00002
Org. Process Res. Dev. 2023, 27, 692−706

in conc. aq. ammonia (25−28 wt %) and reprecipitated using aq. HCl. The InC **2** started to precipitate as dark-colored oily fractions at pH 8.5 but was severely contaminated with the dimer *bis*-**2** (up to 15% by HPLC assay). Fractions collected in the pH range 8.4−6.5 were solid and possessed higher content of the target material. After three consecutive pH-controlled precipitations the overall purity of **2** improved to a sufficient 95.3−95.5% level, with 2.4−2.5% of the dimer *bis*-**2** (HPLC-UV analysis). Additionally, the residual palladium content in the final purified EBL-3183 compound **2** measured by ICP-MS method was found to be 1.294 mg/kg (1.294 ppm).[21]

CONCLUSIONS

In conclusion, we have developed a new synthetic route for the preparation of novel MBL inhibitor pre-candidate **2** in compliance with the scale and purity requirements for preclinical research. The route starts from commercially available indole **3** and employs on Ellman auxiliary approach for introduction of chirality. The key chiral building block **9** was prepared on a kilogram scale in six steps from **3** with an overall yield of 47% (540 g in one batch) with excellent stereoselectivity. The crucial stereoselective preparation of the cyclobutane building block *trans*-**16′** was accomplished by epoxidation of the readily available alkene **13**, followed by scalable separation of the target isomer by crystallization and distillation. The process was carried out in 3 parallel batches with an average yield of 39% (23 g of *trans*-**16′**). As a result, the downstream cyclobutane-containing intermediate nitrile **11′** could be reliably prepared on a sufficient scale (160 g in one batch). Successful implementation of the nitrile reduction step established **11′** as a suitable building block for the synthesis of backup C3-analogues. The final target **2** was prepared in 5 steps from the key intermediate **9** in 29% overall yield on a 100 g scale after concluding ester hydrolysis and scalable purification by pH-controlled precipitation.

METHODS

All commercially available reagents were used as received. Small-scale optimization experiments were carried out under an atmosphere of argon in oven-dried glassware with magnetic stirring. Anhydrous solvents were dispensed by MBRAUN SPS-5 solvent purification system using activated neutral alumina cartridges. ^{1}H, ^{19}F, and proton decoupled ^{13}C{^{1}H} NMR spectra were measured using a 400 MHz Bruker Avance 400 spectrometer at ambient temperature at 400, 376, and 101 MHz, respectively. Chemical shifts are reported in parts per million (ppm) relative to the residual peak of a specified deuterated solvent. Multiplicities are described as follows: br. s (broad singlet), s (singlet), d (doublet), t (triplet), q (quartet), and m (multiplet). Reaction conversions were estimated by LC-MS (Methods A, B) or GC−MS (Method C). LC-MS analyses were performed using a Waters Acquity UPLC H-class instrument (Waters Acquity UPLC BEH-C18 column, 2.1 × 50 mm^2, 1.7 μm, eluent H_2O + 0.1% HCO_2H/MeCN; detection Waters PDA Detector (200−300 nm)). GC−MS analyses were performed using an Agilent 5975C Series GC/MSD instrument (HP-5MS 5% Phenyl Methyl Silox column, 30 m × 250 μm × 0.25 μm, carrier gas helium, flow rate 1 mL/min). High-resolution mass spectra were recorded using a Waters Synapt GII Q-ToF UPLC/MS system. Melting points were determined in open capillaries using an OptiMelt apparatus. Chromatographic purifications were performed using a Buchi Sepacore X10/X50 flash purification system. Compositions of solvent mixtures are indicated either as a volume/volume ratio or as a volume percentage. Optical rotations were measured using an A. Krüss Optronic P3000 polarimeter. ICP-MS analyses were performed by using an Agilent 8900 ICP-QQQ instrument in He mode.

Method A: flow rate 0.8 mL/min; gradient 10−95% over 2.1 min, then 95% over 1.2 min.

Method B: flow rate 0.6 mL/min; gradient 10−95% over 4.1 min, then 95% over 1.8 min.

Method C: temperature gradient 50−275 °C over 15 min.

Ethyl 7-Acetyl-1*H*-indole-2-carboxylate (4). A 25 L glass jacketed reactor equipped with an overhead stirrer, a reflux condenser, and an inert gas inlet/outlet was charged with bromoindole **3** (1.0 kg, 3.73 mol, 1.0 equiv), $Pd(OAc)_2$ (25 g, 0.11 mol, 3 mol %), and dppp (92 g, 0.22 mol, 6 mol %) and purged with nitrogen for 10−15 min. Then, 96% EtOH (7.5 L) was added, and the resulting orange suspension was deoxygenated by three vacuum−nitrogen cycles under stirring. Butyl vinyl ether (1.5 L, 11.59 mol, 3.1 equiv) and Et_3N (1.6 L, 11.20 mol, 3.0 equiv), both prepacked under an inert atmosphere by the vendor, were then added. The obtained dark-orange mixture was brought to 70 ± 5 °C (in jacket, gentle reflux) and maintained at this temperature for 20 h under a constant nitrogen flow. After that time, LC-MS indicated complete consumption of the starting material. The solvent was evaporated under reduced pressure, and the resultant brown residue was redissolved in THF/DCM (2:1; 12 L). The solution was treated with 4 M aq. HCl (4.0 L, 16.0 mol, 4.3 equiv) and stirred at 23 ± 3 °C for 1 h. The resulting brown-orange reaction mixture was diluted with ethyl acetate (10 L), and the layers were separated. The aqueous layer was additionally extracted with EtOAc (2 × 1.0 L); the combined organic phases were washed with H_2O (5.0 L), sat. aq. $NaHCO_3$ (5.0 L), and brine (5.0 L), dried over Na_2SO_4, and then evaporated under reduced pressure. The resulting crude residue (1.08 kg) was redissolved in DCM (5.0 L) and filtered through silica (∼2 kg) on a 5.0 L fritted glass filter eluting with DCM until disappearance of the product in the eluate by TLC-UV. The filtrate was concentrated to a final volume of ∼2 L, diluted with *n*-heptane (1 L), and evaporated further at ≥100 mbar at 35 °C, until most of DCM was removed. The resulting slurry was further diluted with *n*-heptane (1 L). The precipitate was collected on a fritted glass filter, washed with *n*-heptane (3 × 200 mL), and dried under reduced pressure to constant weight to afford **4** (770 g, 3.33 mol, 89% yield) as a bright-yellow solid. ^{1}H NMR (400 MHz, $CDCl_3$) δ 10.80 (br.s, 1H), 7.95−7.91 (m, 1H), 7.91−7.87 (m, 1H), 7.26 (d, J = 2.4 Hz, 1H), 7.21 (dd, J = 7.8, 7.7 Hz, 1H), 4.43 (q, J = 7.1 Hz, 2H), 2.71 (s, 3H), 1.43 (t, J = 7.1 Hz, 3H) ppm. ^{13}C{^{1}H} NMR (101 MHz, $CDCl_3$) δ: 199.8, 161.4, 135.3, 129.4, 129.1, 128.9, 128.2, 121.1, 120.0, 108.4, 61.2, 26.6, 14.5 ppm. LC-MS (ESI$^+$), m/z (I_{rel}, %): 232.2 $[M + H]^+$ (100), t_R = 1.50 min, Method A. HRMS (ESI$^+$) calculated for $C_{13}H_{14}NO_3$ $[M + H]^+$ = 232.0978, observed for $[M + H]^+$ = 232.0974. Melting point: 66.5−67.3 °C.

Ethyl 7-Acetyl-3-bromo-1*H*-indole-2-carboxylate (5). A 25 L glass jacketed reactor equipped with an overhead stirrer, a reflux condenser, and an inert gas inlet/outlet was charged with indole 4 (770 g, 3.33 mol, 1.0 equiv), purged with nitrogen for 10−15 min, and then anhydrous MeCN (10.0 L) was added under stirring. The resulting solution was cooled to 0 ± 3 °C and treated with NBS (623 g, 3.50 mol,

https://doi.org/10.1021/acs.oprd.3c00002
Org. Process Res. Dev. 2023, 27, 692−706

1.05 equiv) in one portion followed by stirring at 23 ± 5 °C for 2.0 h. After that time, LC-MS indicated complete consumption of the starting material. The reaction mixture was quenched with 5% aq. $Na_2S_2O_3$ (10.0 L) and stirred at 23 ± 5 °C for 15 min during which time precipitation occurred. The solids were collected on a fritted glass filter and washed with 50% aq. MeCN (2 × 200 mL) to afford a yellow-green residue (1034 g). Recrystallization of this material from *n*-heptane/EtOAc (10:0.2 L, dilution ∼10:1 v/wt) afforded **5** (970 g, 3.12 mol, 94% yield) as a light-yellow solid. ^{1}H NMR (400 MHz, $CDCl_3$) δ 10.85 (br.s, 1H), 7.97−7.87 (m, 2H), 7.28 (dd, J = 8.1, 7.4 Hz, 1H), 4.47 (q, J = 7.1 Hz, 2H), 2.71 (s, 3H), 1.46 (t, J = 7.1 Hz, 3H) ppm. ^{13}C{^{1}H} NMR (101 MHz, $CDCl_3$) δ 199.7, 160.3, 134.0, 129.30, 129.28, 127.7, 125.8, 121.1, 120.7, 98.6, 61.6, 26.7, 14.5 ppm. LC-MS (ESI$^+$), m/z (I_{rel}, %): 310.1/312.1 $[M + H]^+$ (90), 621.4/625.4 $[2M + H]^+$ (100), t_R = 1.69 min, Method A. HRMS (ESI$^+$) m/z: $C_{13}H_{13}{}^{79}BrNO_3$ $[M + H]^+$ Calculated: 310.0078; Observed: 310.0079. Elemental analysis: $C_{13}H_{12}BrNO_3$ Calculated: C, 50.34; H, 3.90; N, 4.52; Observed: C, 50.42; H, 3.86; N, 4.41. Melting point 87.9−88.5 °C (decomp., *n*-heptane/EtOAc).

Ethyl (*S*)-3-Bromo-7-(1-((*tert*-butylsulfinyl)imino)-ethyl)-1*H*-indole-2-carboxylate ((*S*)-7). A 25 L glass jacketed reactor equipped with an overhead stirrer, a reflux condenser with a Dean−Stark trap, and an inert gas inlet/outlet was charged with ketone **5** (970 g, 3.12 mol, 1.0 equiv) and purged with nitrogen for 15−20 min. Anhydrous THF (5.0 L) was added with stirring, and the resulting solution was treated with (*S*)-*tert*-butanesulfinamide (*S*)-**6** (580 g, 4.78 mol, 1.53 equiv) and $Ti(OEt)_4$ (800 mL, 3.82 mol, 1.22 equiv) at room temperature. The reaction mixture was brought to reflux (∼75 ± 3 °C) with a slow distillation of THF/EtOH azeotrope collecting in the Dean−Stark trap under a constant nitrogen flow. After 16 h, LC-MS monitoring indicated ∼93% conversion. Additional portions of $Ti(OEt)_4$ (150 mL, 0.72 mol, 0.23 equiv) and (*S*)-**6** (50 g, 0.41 mol, 0.15 equiv) were added, and heating was continued for a further 10 h, at which point complete conversion was reached and 1 L of distillate was collected. The reaction mixture was cooled to 50 °C, *N*,*N*,*N*′,*N*′-tetrakis(2-hydroxyethyl)ethylenediamine (THEED, 1200 mL, 5.59 mol, 1.79 equiv) was added, and the reaction mixture was stirred for 45 min at 50 °C. The mixture was diluted with water (4.0 L) and EtOAc (3.0 L) and stirred for 1 h at room temperature. NaCl (4.0 kg) was added to facilitate phase separation (slow, ∼4 h). The aqueous phase was further extracted with EtOAc (2 × 3.0 L), and combined extracts were washed with water (2 × 3.0 L) and dried over Na_2SO_4. Volatiles were evaporated under reduced pressure to yield a dark-green solid, which was purified by filtration through silica (2 × 2.0 kg), eluting with DCM/acetone (15:1). Removal of volatiles from the filtrate afforded (*S*)-**7** (1054 g, 2.55 mol, 82% yield) as a green-gray powder. $[\alpha]_D{}^{20}$ −131 (c 1.0, $CHCl_3$). ^{1}H NMR (400 MHz, $CDCl_3$) δ 11.16 (br. s, 1H), 7.89−7.83 (m, 2H), 7.29 (dd, J = 7.8 Hz, 1H), 4.45 (dq, J = 7.1, 2.0 Hz, 2H), 2.90 (s, 3H), 1.43 (t, J = 7.1 Hz, 3H), 1.41 (s, 9H) ppm. ^{13}C{^{1}H} NMR (101 MHz, $CDCl_3$) δ 178.6, 160.3, 133.6, 129.2, 128.1, 126.7, 125.2, 121.5, 120.9, 98.9, 61.5, 56.8, 22.7, 19.9, 14.5 ppm. LC-MS (ESI$^+$), m/z (I_{rel}, %): 413.1/415.1 $[M + H]^+$ (30), 827.1 $[2M + H]^+$ (100), t_R = 1.73 min, Method A. HRMS (ESI$^+$) m/z: $C_{17}H_{22}{}^{79}BrN_2O_3S$ $[M + H]^+$ Calculated: 413.0535; Observed: 413.0539. Elemental analysis: $C_{17}H_{21}BrN_2O_3S$ Calculated: C, 49.40; H, 5.12; N, 6.78; S, 7.76; Observed C, 49.23; H, 5.17; N, 6.68; S, 7.79. Melting point: 105.3−105.8 °C (decomp., *n*-heptane).

Ethyl 3-Bromo-7-((*S*)-1-(((*S*)-*tert*-butylsulfinyl)amino)-ethyl)-1*H*-indole-2-carboxylate ((*S,S*)-8). A 25 L glass jacketed reactor equipped with an overhead stirrer, a reflux condenser, and an inert gas inlet/outlet was charged with imine (*S*)-**7** (1054 g, 2.55 mol, 1.0 equiv) and purged with nitrogen for 10−15 min. Anhydrous *i*-PrOH (3.5 L) and THF (1.0 L), both prepacked in bottles under an inert atmosphere by the vendor, were added, and (*S*)-**7** was dissolved upon heating to 50 ± 3 °C under constant nitrogen flow. A separate oven-dried 1 L round-bottom flask equipped with a magnetic stirring bar was charged with $[RuCl_2(p\text{-cymene})]_2$ (25.0 g, 0.04 mol, 0.02 equiv) and 2-amino-2-methylpropan-1-ol (8.4 g, 0.09 mol, 0.04 equiv), sealed with a rubber septum, and filled with nitrogen by three vacuum−nitrogen cycles via a needle connection. Upon addition of anhydrous *i*-PrOH (0.7 L), the obtained orange mixture was magnetically stirred at 80 °C for 45 min. After cooling to 40−45 °C, the resulting cherry-red solution was cannulated into the reactor. Next, a separately prepared solution of *t*-BuOK (30.1 g, 0.27 mol, 0.10 equiv) in anhydrous *i*-PrOH (1.0 L) was charged into the reactor by cannulation. The reaction mixture was brought to and maintained at reflux (76−80 °C) for 1 h, at which point LC-MS indicated complete consumption of (*S*)-**7**. The reaction mixture was cooled to room temperature and concentrated to approximately one-half the original volume. The obtained slurry was redissolved in EtOAc (15.0 L) and filtered through a silica plug (2.0 kg). Elution with EtOAc (9−10 L) continued until disappearance of the product in the eluate by TLC-UV. The filtrate was concentrated to a final volume of 3.0 L to afford a thick dark-brown voluminous slurry of crude (*S,S*)-**8**, which was used in the next step without additional purification.

An analytical sample of (*S,S*)-**8** was obtained after evaporation of the crude slurry to dryness and recrystallization of the residue from MeOH/H_2O (3:1, dilution 5:1 v/wt). White powder. $[\alpha]_D{}^{20}$ +120 (c 0.1, $CHCl_3$). ^{1}H NMR (400 MHz, $CDCl_3$) δ 10.98 (br.s, 1H), 7.66 (d, J = 8.2 Hz, 1H), 7.31 (dt, J = 7.3, 1.0 Hz, 1H), 7.19 (dd, J = 8.1, 7.3 Hz, 1H), 4.93 (qd, J = 6.6, 3.3 Hz, 1H), 4.54−4.35 (m, 2H), 3.63 (d, J = 3.4 Hz, 1H), 1.70 (d, J = 6.6 Hz, 3H), 1.44 (t, J = 7.1 Hz, 3H), 1.26 (s, 9H) ppm. ^{13}C{^{1}H} NMR (101 MHz, $CDCl_3$) δ 160.7, 133.3, 129.0, 126.0, 125.1, 123.3, 121.5, 121.0, 98.4, 61.4, 55.6, 50.6, 22.7, 20.8, 14.4 ppm. LC-MS (ESI$^+$), m/z (I_{rel}, %): 415.1/417.1 $[M + H]^+$ (30), 831.3 $[2M + H]^+$ (100), t_R = 1.68 min, Method A. HRMS (ESI$^+$) m/z: $C_{17}H_{24}{}^{79}BrN_2O_3S$ $[M + H]^+$ Calculated: 415.0691; Observed: 415.0687. Melting point: 143.2−144.5 °C (decomp., MeOH/H_2O).

Ethyl (*S*)-7-(1-Aminoethyl)-3-bromo-1*H*-indole-2-carboxylate Hydrochloride (9·HCl). The slurry of crude sulfinamide (*S,S*)-**8** from the previous step (assumed amount: 2.55 mol, 1.0 equiv) containing ∼2 L of EtOAc and/or *i*-PrOH was dissolved in a mixture of EtOH/THF (1:2, 4.5 L) and transferred to a 25 L glass jacketed reactor equipped with an overhead stirrer and an inert gas inlet/outlet. The mixture was cooled to 0 ± 3 °C and treated with 4 M HCl in 1,4-dioxane (1.28 L, 5.12 mol, 2.0 equiv) under stirring. Stirring was continued for 1 h at 23 ± 3 °C under a constant nitrogen flow, upon which time LC-MS indicated complete conversion of the starting material. The reaction mixture was evaporated to dryness under reduced pressure, and the solid residue was diluted with MTBE (4.5 L). The obtained suspension was briefly heated to reflux on a rotovap to extract dark-colored

https://doi.org/10.1021/acs.oprd.3c00002
Org. Process Res. Dev. 2023, 27, 692−706

impurities from the solid. After cooling to room temperature, the mixture was filtered, and the filter cake was thoroughly washed with MTBE (5 × 200 mL). The obtained solid was dried under reduced pressure to constant weight to afford **9**·HCl (702 g, 2.02 mol, 79% yield) as a light-gray powder. $[\alpha]_D^{20}$ +35 (c 1.0, EtOH); Lit:[5] $[\alpha]_D^{20}$ +17 (c 1.0, EtOH). ^{1}H NMR (400 MHz, DMSO-d_6) δ 12.36 (br. S, 1H), 8.79 (br. S, 3H), 7.71−7.65 (m, 1H), 7.59−7.52 (m, 1H), 7.29 (dd, J = 8.1, 7.3 Hz, 1H), 5.29 (dq, J = 6.7, 6.3 Hz, 1H), 4.40 (q, J = 7.1 Hz, 2H), 1.59 (d, J = 6.6 Hz, 3H), 1.38 (t, J = 7.1 Hz, 3H) ppm. ^{13}C{^{1}H} NMR (101 MHz, DMSO-d_6) δ 160.1, 133.3, 127.6, 125.1, 124.9, 123.2, 121.5, 120.3, 96.8, 61.0, 44.6, 20.4, 14.3 ppm. LC-MS (ESI$^+$), m/z (I_{rel}, %): 293.9/295.9 [M − NH_3Cl]$^+$ (100), t_R = 1.25 min, Method A. HRMS (ESI$^+$) m/z: $C_{13}H_{13}NO_2{}^{79}Br$ [M − NH_3Cl]$^+$ Calculated: 294.0130; Observed: 294.0138. Elemental analysis: $C_{13}H_{16}BrClN_2O_2$·0.4H_2O (2 wt % of water) Calculated: C, 44.00; H, 4.77; N, 7.89; Observed: C, 44.23; H, 4.77; N, 7.71. Melting point: 235−238 °C.

Ethyl (*S*)-7-(1-Aminoethyl)-3-bromo-1*H*-indole-2-carboxylate (9). A 25 L glass jacketed reactor equipped with an overhead stirrer, a reflux condenser, and an inert gas inlet/outlet was charged with **9**·HCl (740 g, 2.13 mol, 1.0 equiv) and DCM/H_2O (1:1, 20.0 L) mixture under intense stirring at 23 ± 3 °C. The obtained suspension was treated with solid Na_2CO_3 (1130 g, 10.65 mol, 5.0 equiv) in portions. After complete dissolution (generally within 3−5 h), the lower organic layer was separated and the aqueous phase was further extracted with DCM (2 × 1.0 L). Combined organic phases were washed with brine (1.0 L), dried over Na_2SO_4, and evaporated under reduced pressure to yield 600 g of crude product. This material was recrystallized from *n*-heptane/EtOAc (2.6:0.1 L, dilution 5:1 v/wt) to afford **9** (540 g, 1.74 mol, 86% yield) as a cream solid. $[\alpha]_D^{20}$ +45 (c 1.0, $CHCl_3$). ^{1}H NMR (400 MHz, $CDCl_3$) δ 10.76 (br. s, 1H), 7.59−7.50 (m, 1H), 7.16−7.09 (m, 2H), 4.54 (q, J = 6.6 Hz, 1H), 4.45 (q, J = 7.1 Hz, 2H), 1.66 (br. s, 2H), 1.50 (d, J = 6.6 Hz, 3H), 1.46 (t, J = 7.1 Hz, 3H) ppm. ^{13}C{^{1}H} NMR (101 MHz, $CDCl_3$) δ 161.1, 134.3, 130.0, 128.6, 123.8, 123.3, 121.2, 119.8, 98.0, 61.3, 51.3, 25.2, 14.5 ppm. LC-MS (ESI$^+$), m/z (I_{rel}, %): 294.0/296.0 [M − NH_2]$^+$ (100), t_R = 1.37 min, Method A. HRMS (ESI$^+$) m/z: $C_{13}H_{13}NO_2{}^{79}Br$ [M − NH_2]$^+$ Calculated: 294.0130; Observed: 294.0135. Elemental analysis: $C_{13}H_{15}BrN_2O_2$ Calculated: C, 50.18; H, 4.86; N, 9.00; Observed: C, 50.53; H, 4.87; N, 8.91. Melting point: 105.0−106.1 °C (*n*-heptane/EtOAc).

***Trans*-(*R*,*R*)-1-Oxaspiro[2.3]hexane-5-carbonitrile (*trans*-16′).** A 3.0 L round-bottom flask was charged with *m*-CPBA (70−75%, balance with water, 112 g, 645 mmol, 1.2 equiv) and toluene (1700 mL, dilution 15 mL/g) under magnetic stirring. When most of the solids were dissolved, the mixture was cooled to 0 °C using an ice-water bath. Nitrile **13** (50 g, 537 mmol, 1.0 equiv) was added dropwise to the stirred mixture over 1 h. The reaction mixture was then allowed to warm to room temperature and stirred for 16 h. The reaction was quenched by addition of 5% aq. Na_2SO_3 (400 mL), the organic layer was separated and washed with sat. aq. Na_2CO_3 (3 × 300 mL) and brine (400 mL), and concentrated at 40 °C/40 mbar on a rotovap to an approximate volume of 100 mL. The resulting clear light-yellow oil was diluted with EtOAc (200 mL) and concentrated to the final weight of 66 g. Upon cooling of the obtained solution to −18 ± 2 °C, crystallization occurred. The solid was collected by filtration and washed with cold EtOAc to yield 34 g of material (dr 98:2, 10−15 mol % of EtOAc). Subsequent vacuum distillation (65−75 °C/3 mbar) through a vacuum-jacketed Vigreux column (15 cm) afforded epoxide *trans*-**16′** (13.4 g, 123 mmol, dr 98:2) as a colorless glassy solid. The mother liquor obtained after crystallization was distilled, and the distillate was dissolved in EtOAc (2:1 v/wt) and crystallized at −18 ± 2 °C. Distillation of the crystallized material afforded an additional portion of *trans*-**16′** (9.7 g, 88 mmol, dr >99:1). Total yield 23.1 g (212 mmol, 39.4% yield). Colorless solid. ^{1}H NMR (400 MHz, $CDCl_3$) δ 3.19−3.08 (m, 1H), 2.90−2.81 (m, 2H), 2.79−2.70 (m, 4H) ppm. ^{13}C{^{1}H} NMR (101 MHz, $CDCl_3$) δ 122.3, 57.7, 51.7, 35.7, 15.0 ppm. GC−MS (EI$^+$), m/z (I_{rel}, %): 109.1 [M]$^+$ (5), 79.1 [M − CH_2O]$^+$ (25), 52.1 [M − CH_2O − HCN]$^+$ (100), t_R = 5.15 min, Method C. Melting point: 29.5−32.5 °C.

Ethyl 3-Bromo-7-((*S*)-1-((((1*R*,3*S*)-3-cyano-1-hydroxycyclobutyl)methyl)amino)-ethyl)-1*H*-indole-2-carboxylate (10′). A 2.0 L round-bottom flask equipped with a reflux condenser and a magnetic stirring bar was charged with indole **9** (125.0 g, 402 mmol, 1.0 equiv) and toluene/*t*-AmOH mixture (0.75:0.25 L; dilution 8.0 mL/g). The resulting solution was treated with *trans*-**16′** (dr 98:2, 48.2 g, 442 mmol, 1.1 equiv) in one portion, and the reaction mixture was brought to reflux (120 °C bath temperature). After 18 h of reflux, LC-MS indicated complete consumption of the starting material. The reaction mixture was cooled to room temperature and concentrated under reduced pressure to dryness. The obtained oil was co-evaporated with DCM (3 × 800 mL) to afford 181 g of crude **10′** as a dark-brown oil, which was used in the next step without purification.

An analytical sample was prepared by separation of the crude product mixture using flash chromatography (silica, eluent hexanes/EtOAc, gradient 0−100%) to afford **10′** as a colorless oil. ^{1}H NMR (400 MHz, $CDCl_3$) δ 10.46 (br. s, 1H), 7.61−7.53 (m, 1H), 7.20−7.12 (m, 2H), 4.44 (dq, J = 7.1, 5.1 Hz, 2H), 4.15 (q, J = 6.5 Hz, 1H), 3.20−3.11 (m, 1H), 2.90 (d, J = 12.3 Hz, 1H), 2.62 (d, J = 12.4 Hz, 1H), 2.49−2.27 (m, 4H), 1.50 (d, J = 6.6 Hz, 3H), 1.44 (t, J = 7.1 Hz, 3H) ppm, O*H* and N*H* signals apparently overlap with the broadened H_2O signal. ^{13}C{^{1}H} NMR (101 MHz, $CDCl_3$) δ 161.3, 133.6, 128.7, 128.2, 124.3, 123.7, 122.6, 121.5, 120.3, 98.3, 73.6, 61.5, 58.1, 56.7, 38.5, 38.4, 22.8, 15.3, 14.4 ppm. LC-MS (ESI$^+$), m/z (I_{rel}, %): 294.0/296.0 [M − $C_6H_{10}N_2O$]$^+$ (100), 420.1/422.1 [M + H]$^+$ (15), t_R = 2.61 min, Method B. HRMS (ESI$^+$) m/z: $C_{13}H_{13}{}^{79}BrNO_2$ [M − $C_6H_{10}N_2O$]$^+$ Calculated: 294.0124; Observed: 296.0139.

Ethyl 3-Bromo-7-((*S*)-1-((2*S*,4*R*)-2-cyano-6-oxo-5-oxa-7-azaspiro[3.4]octan-7-yl)ethyl)-1*H*-indole-2-carboxylate (11′). Crude **10′** from the previous stage (181 g; assumed amount: 402 mmol, 1.0 equiv) was dissolved in anhydrous MeCN (1200 mL) in a 4 L round-bottom flask with magnetic stirring. The solution was cooled to 0 °C using an ice-water bath and treated with CDI (181.5 g, 1119 mmol, 2.8 equiv) in one portion. The reaction mixture was stirred at room temperature for 18 h, after which time LC-MS indicated complete consumption of the starting material. The obtained dark-brown solution was diluted with EtOAc (1600 mL) and washed with 1 M aq. HCl (2 × 800 mL). The aqueous layer was extracted with EtOAc (3 × 150 mL). Combined organic extracts were sequentially washed with sat. aq. $NaHCO_3$ (2 × 600 mL), brine (900 mL), dried over Na_2SO_4, then filtered, and evaporated to dryness under reduced pressure. The obtained semisolid residue was suspended in Et_2O (800 mL)

https://doi.org/10.1021/acs.oprd.3c00002
Org. Process Res. Dev. 2023, 27, 692−706

and stirred at room temperature for 17 h. The suspension was filtered, and the solid was washed with Et_2O (3 × 150 mL) and dried under reduced pressure to constant weight to afford **11′** (160 g, 358 mmol, 89% yield) as a gray solid. ^{1}H NMR (400 MHz, $CDCl_3$) δ 10.45 (br. s, 1H), 7.69−7.63 (m, 1H), 7.33−7.27 (m, 1H), 7.21 (dd, J = 8.1, 7.2 Hz, 1H), 5.56 (q, J = 7.1 Hz, 1H), 4.44 (dq, J = 7.1, 1.8 Hz, 2H), 3.73 (d, J = 9.5 Hz, 1H), 3.16 (d, J = 9.5 Hz, 1H), 3.17−3.08 (m, 1H), 2.99−2.88 (m, 1H), 2.86−2.77 (m, 1H), 2.66−2.58 (m, 1H), 2.41−2.33 (m, 1H), 1.74 (d, J = 7.2 Hz, 3H), 1.45 (t, J = 7.1 Hz, 3H) ppm. ^{13}C{^{1}H} NMR (101 MHz, $CDCl_3$) δ 160.4, 157.1, 134.1, 128.6, 125.0, 122.9, 122.8, 121.7, 121.5, 120.9, 98.3, 78.0, 61.5, 50.9, 47.1, 40.6, 39.2, 15.83, 15.2, 14.4 ppm. LC-MS (ESI$^+$), m/z (I_{rel}, %): 294.0/296.0 $[M - C_7H_8N_2O_2]^+$ (100), 446.1/448.1 $[M + H]^+$ (65), t_R = 3.65 min, Method B. HRMS (ESI$^+$) m/z: $C_{20}H_{21}N_3O_4Br$, $[M + H]^+$ Calculated: 446.0715; Observed: 446.0721.

Ethyl 7-((*S*)-1-((2*S*,4*R*)-2-Cyano-6-oxo-5-oxa-7-azaspiro[3.4]octan-7-yl)-ethyl)-3-(3-fluoro-4-(methylsulfonamido)phenyl)-1*H*-indole-2-carboxylate (19). A 2 L round-bottom flask equipped with a reflux condenser, an overhead stirrer, and an inert gas inlet/outlet was charged with bromide **11′** (83.5 g, 187 mmol, 1.0 equiv), boronate **17** (76.6 g, 243 mmol, 1.3 equiv) and $Pd(dppf)Cl_2 \cdot CH_2Cl_2$ (7.64 g, 9 mmol, 5 mol %). Next 1,4-dioxane (1.14 L; 13.7 mL/g) was added followed by a solution of Na_2CO_3 (79.3 g, 748 mmol, 4 equiv) in H_2O (280 mL). The resulting mixture was deoxygenated by bubbling argon through a needle for at least 20 min. The reaction mixture was brought to 80 °C (bath temperature) and heated at this temperature for 3.5 h under a constant argon flow. At this point, LC-MS indicated complete conversion of the starting material. Upon cooling to 40−45 °C, the mixture was quenched[22] with a solution of APDTC (4.6 g, 0.15 equiv) in water (170 mL) and stirred at 40 °C for 45 min. Upon cooling to room temperature, the reaction mixture was partitioned between EtOAc (800 mL) and water (1000 mL). The separated aqueous layer was extracted with EtOAc (2 × 500 mL), combined organic phases were washed with H_2O (3 × 800 mL), filtered through a Celite plug, and concentrated to a final volume of ∼500 mL. Precipitated solids were removed by filtration, washed with EtOAc (3 × 60 mL), and dried under reduced pressure to constant weight to afford **19** (74.3 g, 134 mmol, 72% yield) as a light-gray powder. $[\alpha]_D^{20}$ +134 (c 1.0, $CHCl_3$). ^{1}H NMR (400 MHz, $CDCl_3$) δ 10.46 (br. s, 1H), 7.68−7.58 (m, 2H), 7.43−7.35 (m, 2H), 7.34−7.29 (m, 1H), 7.17 (dd, J = 8.2, 7.2 Hz, 1H), 6.66 (br. s, 1H), 5.61 (q, J = 7.1 Hz, 1H), 4.34 (q, J = 7.1 Hz, 2H), 3.77 (d, J = 9.6 Hz, 1H), 3.23 (d, J = 9.6 Hz, 1H), 3.20−3.12 (m, 1H), 3.11 (s, 3H), 3.01−2.92 (m, 1H), 2.90−2.81 (m, 1H), 2.68−2.61 (m, 1H), 2.44−2.37 (m, 1H), 1.77 (d, J = 7.2 Hz, 3H), 1.35 (t, J = 7.1 Hz, 3H) ppm. ^{13}C{^{1}H} NMR (101 MHz, $CDCl_3$) δ 161.1, 157.2, 153.5 (d, J_{FC} = 243.5 Hz), 134.4, 132.2 (d, J_{FC} = 8.1 Hz), 128.1, 127.4 (d, J_{FC} = 3.3 Hz), 123.9, 123.6 (d, J_{FC} = 12.6 Hz), 122.7, 122.51, 122.50, 122.1 (d, J_{FC} = 1.9 Hz), 121.7, 121.5, 120.8, 118.1 (d, J_{FC} = 20.2 Hz), 78.0, 61.2, 51.0, 47.4, 40.6, 40.0, 39.2, 15.9, 15.2, 14.3 ppm. LC-MS (ESI$^+$), m/z (I_{rel}, %): 555.1 $[M + H]^+$ (100), t_R = 3.08 min, Method B. HRMS (ESI$^+$) m/z: $C_{27}H_{28}N_4O_6FS$ $[M + H]^+$ Calculated: 555.1714; Observed: 555.1721.

Ethyl 7-((*S*)-1-((2*S*,4*R*)-2-(Aminomethyl)-6-oxo-5-oxa-7-azaspiro[3.4]-octan-7-yl)ethyl)-3-(3-fluoro-4-(methylsulfonamido)phenyl)-1*H*-indole-2-carboxylate (20). A 1 L Hastelloy autoclave equipped with a mechanical stirrer was charged with the nitrile **19** (20.0 g, 36.1 mmol, 1.0 equiv), THF (600 mL, dilution 30 mL/g), and conc. aq. NH_4OH (25−28 wt %) (200 mL, dilution 10 mL/g). The resulting biphasic mixture was supplemented with Raney-Ni (15 mL, ∼10 g, 50 wt %) and hydrogenated under 50 bar pressure at 50 °C, over 18 h. After that time, LC-MS analysis indicated complete consumption of the starting material. Upon cooling to room temperature, the catalyst was filtered off using Celite and washed with THF (3 × 30 mL). The filtrate was evaporated under reduced pressure, the green oily residue was diluted with EtOH (100 mL), and the obtained mixture was briefly brought to reflux with stirring. Upon cooling to room temperature, the precipitated solids were filtered off and rinsed with EtOH (2 × 30 mL) to afford the amine **20** (13.0 g, 23.3 mmol, 65% yield) as a white powder. $[\alpha]_D^{20}$ +115 (c 1.0, DMSO). ^{1}H NMR (400 MHz, DMSO-d_6) δ 7.49 (dd, J = 8.2, 1.0 Hz, 1H), 7.40 (dd, J = 8.7, 8.7 Hz, 1H), 7.33−7.29 (m, 1H), 7.26 (dd, J = 12.2, 2.0 Hz, 1H), 7.20−7.15 (m, 1H), 7.11 (dd, J = 8.2, 7.2 Hz, 1H), 5.55 (q, J = 7.0 Hz, 1H), 4.24 (q, J = 7.1 Hz, 2H), 3.74 (d, J = 9.6 Hz, 1H), 3.29 (d, J = 9.6 Hz, 1H), 2.90 (s, 3H), 2.71−2.66 (m, 2H), 2,48−2.41 (m, 1H), 2.40−2.29 (m, 2H), 2.18−2.09 (m, 1H), 2.05−1.94 (m, 1H), 1.62 (d, J = 7.0 Hz, 3H), 1.21 (t, J = 7.1 Hz, 3H) ppm, exchangeable NH_2, indole and sulfonamide NH signals were not detected. ^{13}C{^{1}H} NMR (101 MHz, DMSO-d_6) δ 161.0, 156.7, 154.5 (d, J_{FC} = 242.1 Hz), 133.9, 130.1 (d, J_{FC} = 11.6 Hz), 127.4, 127.0 (d, J_{FC} = 8.0 Hz), 126.3 (d, J_{FC} = 2.8 Hz), 125.2, 123.0, 122.8 (d, J_{FC} = 2.4 Hz), 122.1 (d, J_{FC} = 1.9 Hz), 122.0, 120.7, 120.4, 117.5 (d, J_{FC} = 20.9 Hz), 78.5, 60.4, 52.1, 47.0, 44.8, 37.6, 37.1, 27.1, 17.0, 13.9 ppm, signal of CH_3SO_2NH (39.3 ppm according to HSQC experiment) overlaps with DMSO-d_6 signal. LC-MS (ESI$^+$), m/z (I_{rel}, %): 559.3 $[M + H]^+$ (100), t_R = 1.38 min, Method A. HRMS (ESI$^+$) m/z: $C_{27}H_{32}N_4O_6FS$ $[M + H]^+$ Calculated: 559.2027; Observed: 559.2032. Melting point: >260 °C.

7-((*S*)-1-((2*S*,4*R*)-2-(Aminomethyl)-6-oxo-5-oxa-7-azaspiro[3.4]octan-7-yl)ethyl)-3-(3-fluoro-4-(methylsulfonamido)phenyl)-1*H*-indole-2-carboxylic Acid (2). In a 2 L round-bottom flask, ester **20** (110 g, 198 mmol, 1.0 equiv) was suspended in a mixture of THF/H_2O (0.8:0.3 L, dilution 10 mL/g) under magnetic stirring and the mixture was cooled to 0 °C using ice-water bath. A solution of $LiOH \cdot H_2O$ (42 g, 595 mmol, 3.0 equiv) in H_2O (250 mL) was added dropwise over 1 h under vigorous stirring. The mixture was allowed to warm to room temperature and stirred for 40 h with LC-MS monitoring. Upon consumption of the starting material, the reaction mixture was filtered through a Celite plug. The filter cake was washed with 50% aq. THF (3 × 50 mL), the combined filtrates (pH ∼11) were acidified with glacial AcOH to pH 6.0 at room temperature, and the resulting slurry was aged for 0.5 h. The obtained precipitate was collected by filtration, washed with H_2O to neutrality, and dried under reduced pressure to yield ∼100 g of crude **2** (HPLC-UV assay: 85−87% content). Subsequent purification by pH-controlled precipitation and antisolvent precipitation was performed as follows.

pH-Controlled Precipitation. Crude **2** (total 162 g from combined batches of similar quality, estimated quantity: 140 g, 264 mmol) was dissolved in conc. aq. NH_4OH (25−28 wt %, 1000 mL, dilution ∼6:1 mL/g) with gentle heating. The obtained solution was slowly treated with aq. HCl under pH control at room temperature under stirring. 6 M aq. HCl was

https://doi.org/10.1021/acs.oprd.3c00002
Org. Process Res. Dev. 2023, 27, 692−706

used within the pH range 11.5−9.0, whereas 1 M aq. HCl was used within the 9.0−6.5 range. Precipitation started at pH 8.5 with the formation of dark-colored oily fractions (*bis*-**2** content up to 15 area%), which were discarded by decantation. Solid fractions formed at pH range 8.4−6.5 were collected by filtration, washed with H_2O, and dried to constant weight under reduced pressure to afford 130 g of material (90−93% content of **2**, 3.5−4% content of *bis*-**2**).

Antisolvent Precipitation. Material obtained by pH-controlled precipitation (130 g) was dissolved in 50% aq. AcOH (800 mL, 6:1 v/wt) with gentle heating. The solution was concentrated under reduced pressure to an ∼200 mL volume. The resulting amber-colored viscous semisolid mass was diluted with an equal volume of H_2O (200 mL) and dissolved upon gentle heating. The stirred solution was treated dropwise with EtOH (∼450 mL) at room temperature. The precipitated material was collected by filtration and dried to constant weight under reduced pressure to afford 104 g of a stable solvate **2**·0.75EtOH (94.9−95.1% content of **2**, 3.1% content of *bis*-**2**).

The final pH-controlled precipitation was performed as described above to afford **2** (98 g, 184.7 mmol, 69.9% yield) as a white crystalline powder. Attained purity: 95.3−95.5%, *bis*-**2** content: 2.4−2.5% by HPLC-UV (210, 254 nm). $[\alpha]_D^{20}$ +84 (c 1.0, DMSO). ^{1}H NMR (400 MHz, DMSO-d_6) δ 10.34 (br. s, 1H), 8.66 (br. s, 3H), 7.5−7.4 (m, 2H), 7.4−7.3 (m, 2H), 7.1 (d, J = 7.2 Hz, 1H), 7.0 (t, J = 7.7 Hz, 1H), 5.4 (q, J = 7.0 Hz, 1H), 3.7 (d, J = 9.7 Hz, 1H), 3.1 (d, J = 9.7 Hz, 1H), 3.1 (s, 3H), 2.9−2.7 (m, 2H), 2.6−2.5 (m, 1H), 2.5−2.4 (m, 1H), 2.4−2.3 (m, 1H), 2.2 (dd, J = 12.6, 5.9 Hz, 1H), 2.0 (dd, J = 12.9, 6.0 Hz, 1H), 1.6 (d, J = 7.0 Hz, 3H) ppm, sulfonamide N*H* signal was not detected. ^{1}H NMR (400 MHz, CD_3CO_2D) δ 7.6 (t, J = 8.4 Hz, 1H), 7.6 (d, J = 8.2 Hz, 1H), 7.4 (dd, J = 11.5, 1.9 Hz, 1H), 7.4−7.4 (m, 2H), 7.2 (dd, J = 8.1, 7.3 Hz, 1H), 5.6 (q, J = 7.0 Hz, 1H), 3.7 (d, J = 9.7 Hz, 1H), 3.2 (d, J = 9.7 Hz, 1H), 3.2−3.1 (m, 5H), 2.8−2.6 (m, 2H), 2.6−2.5 (m, 1H), 2.3−2.2 (m, 1H), 2.0−1.9 (m, 1H), 1.8 (d, J = 7.1 Hz, 3H) ppm, exchangeable CO_2H, NH_2, indole and sulfonamide N*H* signals were not detected. ^{13}C{^{1}H} NMR (101 MHz, CD_3CO_2D) δ 166.2, 159.6, 155.4 (d, J_{FC} = 244.2 Hz), 135.7, 133.3 (d, J_{FC} = 8.0 Hz), 128.9, 128.0 (d, J_{FC} = 3.1 Hz), 125.1, 124.9 (d, J_{FC} = 13.0 Hz), 124.5, 124.1 (d, J_{FC} = 1.8 Hz), 123.9, 123.8, 122.3, 121.9, 119.0 (d, J_{FC} = 20.7 Hz), 80.6, 51.9, 48.2, 45.1, 40.3, 39.3, 38.5, 26.2, 15.9 ppm. ^{19}F NMR (376 MHz, CD_3CO_2D) δ −128.3 (dd, J = 11.4, 8.6 Hz) ppm. LC-MS (ESI$^+$), m/z (I_{rel}, %): 531.3 $[M + H]^+$ (100), t_R = 1.15 min, Method A. HRMS (ESI$^+$) m/z: $C_{25}H_{28}N_4O_6FS$ $[M + H]^+$ Calculated: 531.1714; Observed: 531.1717. Elemental analysis: $C_{25}H_{27}FN_4O_6S$·0.75H_2O (2.3 wt % of water) Calculated: C, 55.19; H, 5.28; N, 10.30; S, 5.89; Observed: C, 55.19; H, 5.00; N, 10.35; S, 5.86. HPLC-UV Purity: 95.3% (210 nm); 95.5% (254 nm). Melting point: >260 °C.

■ ASSOCIATED CONTENT

Supporting Information

The Supporting Information is available free of charge at https://pubs.acs.org/doi/10.1021/acs.oprd.3c00002.

Graphical and numerical representations of ^{1}H and ^{13}C{^{1}H} spectra for all synthesized compounds, preliminary optimization experiments, HPLC chromatograms for *trans*-**16** and **2**, GC−MS chromatogram for the *trans*/*cis*-**16**′ mixture, and ICP-MS data for the purified compound **2** (PDF)

■ AUTHOR INFORMATION

Corresponding Authors

Andrei Baran − *Latvian Institute of Organic Synthesis, Riga LV-1006, Latvia;* orcid.org/0000-0002-9383-8472; Email: baran.andrei@gmail.com

Christopher J. Schofield − *Chemistry Research Laboratory, Department of Chemistry and the Ineos Oxford Institute for Antimicrobial Research, University of Oxford, Oxford OX1 3TA, United Kingdom;* orcid.org/0000-0002-0290-6565; Email: christopher.schofield@chem.ox.ac.uk

Kirill Shubin − *Latvian Institute of Organic Synthesis, Riga LV-1006, Latvia*; Email: kir101@osi.lv

Authors

Jevgenijs Kuzmins − *Latvian Institute of Organic Synthesis, Riga LV-1006, Latvia*

Jevgenijs Kuznecovs − *Latvian Institute of Organic Synthesis, Riga LV-1006, Latvia*

Alistair J. M. Farley − *Chemistry Research Laboratory, Department of Chemistry and the Ineos Oxford Institute for Antimicrobial Research, University of Oxford, Oxford OX1 3TA, United Kingdom;* orcid.org/0000-0001-5578-6790

Tharindi Panduwawala − *Chemistry Research Laboratory, Department of Chemistry and the Ineos Oxford Institute for Antimicrobial Research, University of Oxford, Oxford OX1 3TA, United Kingdom*

Anete Parkova − *Latvian Institute of Organic Synthesis, Riga LV-1006, Latvia*

Pavel A. Donets − *Latvian Institute of Organic Synthesis, Riga LV-1006, Latvia*

Jürgen Brem − *Chemistry Research Laboratory, Department of Chemistry and the Ineos Oxford Institute for Antimicrobial Research, University of Oxford, Oxford OX1 3TA, United Kingdom;* Present Address: Janssen Research & Development, Janssen Pharmaceutica, B-2340 Beerse, Belgium; orcid.org/0000-0002-0137-3226

Edgars Suna − *Latvian Institute of Organic Synthesis, Riga LV-1006, Latvia;* orcid.org/0000-0002-3078-0576

Complete contact information is available at: https://pubs.acs.org/10.1021/acs.oprd.3c00002

Author Contributions

The manuscript was written through contributions of all authors. All authors have given approval to the final version of the manuscript.

Funding

Research was conducted as part of the ND4BB European Gram-Negative Antibacterial Engine (ENABLE) Consortium (www.nd4bb-enable.eu) and has received funding from the Innovative Medicines Initiative Joint Undertaking under Grant Agreement No. 115583, resources of which are composed of a financial contribution from the European Union's Seventh Framework Programme (FP7/2007-2013) and The European Federation of Pharmaceutical Industries and Associations (EFPIA) companies' kind contribution. The ENABLE project was also financially supported by contributions from Academic and small and medium-sized enterprise (SME) partners.

Notes

The authors declare no competing financial interest.

■ ABBREVIATIONS

AD-mix (α or β), commercial oxidant mixture containing potassium osmate, potassium ferricyanide, potassium carbonate and $(DHQ/DHQD)_2PHAL$ chiral ligands; APDTC, ammonium pyrrolidine-1-carbodithioate; Cbz, benzyloxycarbonyl; CDI, 1,1′-carbonyldiimidazole; Celite, naturally occurring diatomaceous earth; *m*-CPBA, 3-chloroperbenzoic acid; DCM, dichloromethane; dppp, 1,3-bis(diphenylphosphino)-propane; EI, electron ionization, formerly electron impact ionization; Ellman's sulfinamide, *tert*-butanesulfinamide; D-epoxone, 1,2:4,5-di-*O*-isopropylidene-β-D-erythro-2,3-hexodiulo-2,6-pyranose; ESI, electrospray ionization; ESKAPE, antibiotic-resistant bacterial pathogens including *Enterococcus faecium*, *Staphylococcus aureus*, *Klebsiella pneumoniae*, *Acinetobacter baumannii*, *Pseudomonas aeruginosa*, and *Enterobacter* spp.; GC−MS, gas chromatography−mass spectrometry; HPLC, high-performance liquid chromatography; HRMS, high-resolution mass spectrometry; ICH, International Council for Harmonisation of Technical Requirements for Pharmaceuticals for Human Use; ICP-MS, inductively coupled plasma mass spectrometry; IMP, imipenemase-type metallo-β-lactamase; InC, indole carboxylate; L-selectride, lithium tri-*sec*-butylborohydride; MBLs, metallo-β-lactamases; MTBE, methyl *tert*-butyl ether; NBS, *N*-bromosuccinimide; NDM, New Delhi metallo-β-lactamase; NMR, nuclear magnetic resonance; Oxone, potassium peroxymonosulfate; $Pd(dppf)Cl_2{\cdot}CH_2Cl_2$, [1,1′-bis(diphenylphosphino)ferro-cene]dichloro-palladium-(II), complex with dichloromethane; PDA, photodiode array; PDE, permitted daily exposure; Q-ToF, quadrupole time-of-flight mass spectrometry; Raney-Ni, Raney nickel; t_R, retention time; THF, tetrahydrofuran; THEED, *N,N,N′,N′*-tetrakis(2-hydroxyethyl)ethylenediamine; TLC, thin-layer chromatography; TsCl, 4-toluenesulfonyl chloride; UPLC, ultraperformance liquid chromatography; UV, ultraviolet; VIM, Verona integron-encoded metallo-β-lactamase

■ REFERENCES

(1) (a) Cantón, R.; Gijón, D.; Ruiz-Garbajosa, P. Antimicrobial Resistance in ICUs: An Update in the Light of the COVID-19 Pandemic. *Curr. Opin. Crit. Care* **2020**, *26*, 433−441. (b) Ma, Y.; Wang, C.; Li, Y.; Li, J.; Wan, Q.; Chen, J.; Tay, F. R.; Niu, L. Considerations and Caveats in Combating ESKAPE Pathogens against Nosocomial Infections. *Adv. Sci.* **2020**, *7*, No. 1901872. (c) De Oliveira, D. M. P.; Forde, B. M.; Kidd, T. J.; Harris, P. N. A.; Schembri, M. A.; Beatson, S. A.; Paterson, D. L.; Walker, M. J. Antimicrobial Resistance in ESKAPE Pathogens. *Clin. Microbiol. Rev.* **2020**, *33*, No. e00181-19.

(2) (a) Bonomo, R. A.; Burd, E. M.; Conly, J.; Limbago, B. M.; Poirel, L.; Segre, J. A.; Westblade, L. F. Carbapenemase-Producing Organisms: A Global Scourge. *Clin. Infect. Dis.* **2018**, *66*, 1290−1297. (b) Palacios-Baena, Z. R.; Giannella, M.; Manissero, D.; Rodríguez-Baño, J.; Viale, P.; Lopes, S.; Wilson, K.; McCool, R.; Longshaw, C. Risk Factors for Carbapenem-Resistant Gram-Negative Bacterial Infections: A Systematic Review. *Clin. Microbiol. Infect.* **2021**, *27*, 228−235. (c) Nordmann, P.; Poirel, L. Epidemiology and Diagnostics of Carbapenem Resistance in Gram-Negative Bacteria. *Clin. Infect. Dis.* **2019**, *69*, S521−S528.

(3) (a) De Angelis, G.; Del Giacomo, P.; Posteraro, B.; Sanguinetti, M.; Tumbarello, M. Molecular Mechanisms, Epidemiology, and Clinical Importance of β-Lactam Resistance in Enterobacteriaceae. *Int. J. Mol. Sci.* **2020**, *21*, 5090. (b) Palzkill, T. Metallo-β-Lactamase Structure and Function: Metallo-β-Lactamase Structure and Function. *Ann. N. Y. Acad. Sci.* **2013**, *1277*, 91−104.

(4) Brem, J.; Panduwawala, T.; Hansen, J. U.; Hewitt, J.; Liepins, E.; Donets, P.; Espina, L.; Farley, A. J. M.; Shubin, K.; Campillos, G. G.; Kiuru, P.; Shishodia, S.; Krahn, D.; Leśniak, R. K.; Schmidt, J.; Calvopiña, K.; Turrientes, M.-C.; Kavanagh, M. E.; Lubriks, D.; Hinchliffe, P.; Langley, G. W.; Aboklaish, A. F.; Eneroth, A.; Backlund, M.; Baran, A. G.; Nielsen, E. I.; Speake, M.; Kuka, J.; Robinson, J.; Grinberga, S.; Robinson, L.; McDonough, M. A.; Rydzik, A. M.; Leissing, T. M.; Jimenez-Castellanos, J. C.; Avison, M. B.; Da Silva Pinto, S.; Pannifer, A. D.; Martjuga, M.; Widlake, E.; Priede, M.; Hopkins Navratilova, I.; Gniadkowski, M.; Belfrage, A. K.; Brandt, P.; Yli-Kauhaluoma, J.; Bacque, E.; Page, M. G. P.; Björkling, F.; Tyrrell, J. M.; Spencer, J.; Lang, P. A.; Baranczewski, P.; Cantón, R.; McElroy, S. P.; Jones, P. S.; Baquero, F.; Suna, E.; Morrison, A.; Walsh, T. R.; Schofield, C. J. Imitation of β-Lactam Binding Enables Broad-Spectrum Metallo-β-Lactamase Inhibitors. *Nat. Chem.* **2022**, *14*, 15−24.

(5) Schofield, C.; Brem, J.; Panduwawala, T.; Farley, A.; Suna, E. 2-Carboxyl-Indole Inhibitors Of Metallo-Beta-Lactamases. WIPO Patent WO2022/248887A1, 2022.

(6) (a) Adamkiewicz, A.; Mlynarski, J. Diastereoselective Hydrosilylation of *N*-(*Tert*-Butylsulfinyl)Imines Catalyzed by Zinc Acetate. *Eur. J. Org. Chem.* **2016**, *2016*, 1060−1065. (b) Li, Z.; Deng, G.; Li, Y.-C. Zinc(II) Iodide-Triethylsilane: A Novel Mild Reduction System for Direct Deoxygenation of Aryl Aldehydes, Ketones, and α,β-Unsaturated Enones. *Synlett* **2008**, *2008*, 3053−3057.

(7) (a) Guijarro, D.; Pablo, Ó.; Yus, M. Achiral β-Amino Alcohols as Efficient Ligands for the Ruthenium-Catalysed Asymmetric Transfer Hydrogenation of Sulfinylimines. *Tetrahedron Lett.* **2011**, *52*, 789−791. (b) Guijarro, D.; Pablo, Ó.; Yus, M. Synthesis of Highly Enantiomerically Enriched Amines by Asymmetric Transfer Hydrogenation of N-(Tert-Butyl-sulfinyl)Imines. *Org. Synth.* **2013**, *90*, 338. (c) Guijarro, D.; Pablo, Ó.; Yus, M. Synthesis of γ-, δ-, and ϵ-Lactams by Asymmetric Transfer Hydrogenation of *N*-(*Tert*-Butylsulfinyl)-Iminoesters. *J. Org. Chem.* **2013**, *78*, 3647−3654.

(8) (a) Han, Z.; Koenig, S. G.; Zhao, H.; Su, X.; Singh, S. P.; Bakale, R. P. Development of a Large-Scale Stereoselective Process for (1*R*,4*S*)-4-(3,4-Dichlorophenyl)-1,2,3,4-Tetrahydronaphthalen-1-Amine Hydrochloride. *Org. Process Res. Dev.* **2007**, *11*, 726−730. (b) Tabet, S.; Rodeville, N.; Boiteau, J.-G.; Cardinaud, I. Improved Process for Preparation of *Tert*-Butanesulfinyl Ketimines of Hindered Ketones under Nitrogen Flow. *Org. Process Res. Dev.* **2016**, *20*, 1383−1387. (c) Tabet, S.; Rodeville, N.; Mathieu, A.; Raffin, C.; Millois-Barbuis, C.; Musicki, B.; Muller, F.; Gerfaud, T.; Boiteau, J.-G.; Cardinaud, I. Early Development Scale-Up of a Novel CXCR Antagonist: Focus on Racemic and Stereoselective Routes of a Key Intermediate. *Org. Process Res. Dev.* **2017**, *21*, 2032−2044.

(9) Brunner, E.; Scholz, A. G. R. Isobaric Vapor-Liquid Equilibria of the Tetrahydro-furan/Ethanol System at 25, 50, and 100 KPa. *J. Chem. Eng. Data* **1984**, *29*, 28−31.

(10) Reeves, J. T.; Tan, Z.; Han, Z. S.; Li, G.; Zhang, Y.; Xu, Y.; Reeves, D. C.; Gonnella, N. C.; Ma, S.; Lee, H.; Lu, B. Z.; Senanayake, C. H. Direct Titanium-Mediated Conversion of Ketones into Enamides with Ammonia and Acetic Anhydride. *Angew. Chem., Int. Ed.* **2012**, *51*, 1400−1404.

(11) See Supporting Information, pages S17 and S18 for details.

(12) Caserio, F. F., Jr.; Parker, S. H.; Piccolini, R.; Roberts, J. D. Small-ring Compounds. XX. 1,3-Dimethylenecyclobutane and Related Compounds. *J. Am. Chem. Soc.* **1958**, *80*, 5507−5513.

(13) Razin, V. V.; Ulin, N. V. Prototropic Isomerization of 1-Oxaspiro[2.3]Hexane-5-Carbonitrile and Methyl 1-Oxaspiro[2.3]-Hexane-5-Carboxylate into the Corresponding 3-Hydroxymethylbicyclo[1.1.0]Butane-1-Carboxylic Acid Derivatives. *Russ. J. Org. Chem.* **2003**, *39*, 33−39.

(14) See Supporting Information, page S27 for details.

(15) Giraudeau, P.; Baguet, E. Improvement of the Inverse-Gated-Decoupling Sequence for a Faster Quantitative Analysis of Various Samples by ^{13}C NMR Spectroscopy. *J. Magn. Reson.* **2006**, *180*, 110−117.

(16) See Supporting Information, pages S26 and S27 for details.

(17) See Supporting Information, pages S32 and S33 for details.

(18) See Supporting Information, pages S39−S42 for details.

https://doi.org/10.1021/acs.oprd.3c00002
Org. Process Res. Dev. 2023, 27, 692−706

(19) See Supporting Information, pages S45 and S46 for details.
(20) Lu, Q.; Liu, J.; Ma, L. Recent Advances in Selective Catalytic Hydrogenation of Nitriles to Primary Amines. *J. Catal.* **2021**, *404*, 475−492.
(21) See Supporting Information, page S58 for details. According to ICH guidelines Q3D Step 5, page 62, the content of palladium as Class 2B elemental impurity should not exceed 20 ppm in API for oral exposure, and 2 ppm for parenteral exposure based on a maximum daily dose of 5 g of drug/day.
(22) Gallagher, W. P.; Vo, A. Dithiocarbamates: Reagents for the Removal of Transition Metals from Organic Reaction Media. *Org. Process Res. Dev.* **2015**, *19*, 1369−1373.

https://doi.org/10.1021/acs.oprd.3c00002
Org. Process Res. Dev. 2023, 27, 692−706